Nonlinear Dynamics **8:** 315–346, 1995.

Non-Linear Normal Modes, Invariance, and Modal Dynamics Approximations of Non-Linear Systems

NICOLAS BOIVIN, CHRISTOPHE PIERRE, and STEVEN W. SHAW
Department of Mechanical Engineering and Applied Mechanics, 2250 G.G. Brown Building, The University of Michigan, Ann Arbor, MI 48109-2125, U.S.A.

(Received: 14 August 1993; accepted: 26 July 1994)

Abstract. Non-linear systems are here tackled in a manner directly inherited from linear ones, that is, by using proper normal modes of motion. These are defined in terms of invariant manifolds in the system's phase space, on which the uncoupled system dynamics can be studied. Two different methodologies which were previously developed to derive the non-linear normal modes of continuous systems – one based on a purely continuous approach, and one based on a discretized approach to which the theory developed for discrete systems can be applied – are simultaneously applied to the same study case – an Euler–Bernoulli beam constrained by a non-linear spring – and compared as regards accuracy and reliability. Numerical simulations of pure non-linear modal motions are performed using these approaches, and compared to simulations of equations obtained by a classical projection onto the linear modes. The invariance properties of the non-linear normal modes are demonstrated, and it is also found that, for a pure non-linear modal motion, the invariant manifold approach achieves the same accuracy as that obtained using several linear normal modes, but with significantly reduced computational cost. This is mainly due to the possibility of obtaining high-order accuracy in the dynamics by solving only one non-linear ordinary differential equation.

Key words: Non-linear normal modes, non-linear modal dynamics, invariant manifolds.

1. Introduction

The concept of normal modes of motion is well developed for linear oscillatory systems, due to the special features of the linear differential equations governing their dynamics. These features allow for a definition of normal modes in terms of eigenvectors (or eigenfunctions) and the expression of an arbitrary system response as a superposition of modal responses (see, for example, [1]). A normal mode motion for a linear oscillatory system is one which is analogous to that of an equivalent single-degree of freedom oscillator, and which takes place on a (two-dimensional) plane in the system's phase space.

It is evident that no complete analogy of linear modal analysis can exist for non-linear systems, simply because superposition does not hold. However, many of the relevant ideas can be generalized. For example, much work has been done on the existence and stability of normal modes of motion for two-degree of freedom, conservative systems (see, for example, [2–4]). The purpose of the methodologies developed in [5–8] was to generalize these definitions to a very wide class of systems which includes non-conservative, gyroscopic, and infinite-dimensional systems. In particular, these results include (1) a definition of normal modes for a general class of non-linear systems, (2) constructive techniques for obtaining these modes for weakly non-linear systems and, (3) means of generating the differential equations which govern the dynamics of the system when it is undergoing a non-linear normal mode motion. Moreover, these developments clearly demonstrate the origins of the usual normal modes which exist in linearized systems.

In order to extend modal analysis ideas to non-linear systems – which is the ultimate goal of this line of research – an approach which is fundamentally different from the usual separation of variables and resulting eigenvalue problem must be adopted. Such an approach is offered by defining normal modes in terms of motions which occur on low – typically two – dimensional invariant manifolds in the system's phase space. Such a motion must be inherently like that of a lower dimensional system, and this is exactly what is desired for a normal mode motion. A constructive technique for generating such manifolds in terms of asymptotic series, without having to solve the equations of motion, is provided by a simple generalization of the method used in constructing approximate center manifolds in bifurcation theory (see [9]). Using this approach, it is possible to determine the manifolds which represent the normal modes for weakly non-linear systems. The equations of motion restricted to these manifolds then provide the dynamics of the associated normal modes. Along the same line, some recent advances include the treatment of strongly non-linear discrete systems, mode localization for multi-degree of freedom non-linear systems with cyclic symmetries, and systems with internal resonances (see [10–12]).

For oscillatory systems, the invariant manifolds are two-dimensional and the modal dynamics on them are governed by second-order, non-linear oscillator equations. From these manifolds, one can deduce the physical behavior of the system undergoing a purely modal motion and, in particular, the amplitude-dependent mode shapes can be obtained. From the non-linear modal oscillators, one can obtain information about the amplitude-dependent frequencies and the amplitude decay rates. For an N-degree of freedom system (N finite or infinite) there exists N such normal mode manifolds (under certain non-degeneracy conditions). The tangent planes to these manifolds at the equilibrium point are the planes on which the usual modal dynamics of the linearized system take place, i.e., they are the familiar eigenspaces.

By definition, these non-linear normal mode manifolds are invariant, so that any motion starting exactly in one non-linear normal mode will be comprised only of that mode for all time, and will not generate any motion in the other non-linear normal modes. On the contrary, a standard linear modal analysis of the system's dynamics on that same manifold – obtained by mere projection of the equations of motion onto the linear modes – would produce a two-way exchange of energy, or "contamination", between the linear mode tangent to the manifold on which the motion is initiated and the other linear modes, due to the non-linear coupling terms between the projected equations obtained. (Note, these are linearly uncoupled if one projects on the exact linear modes). As will be demonstrated (see Section 3.4), this may yield inaccurate results if one includes only few linear modes, or expensive solutions if one includes many of them.

To date, two different but consistent invariant manifold methodologies have been developed to determine the non-linear normal modes of continuous systems and the attendant dynamics: the first one – reviewed in Section 2.1 – treats continuous systems as such, so that the non-linear normal modes are directly obtained from the partial differential equation of motion (see [6]), while the second one – reviewed in Section 2.2 – first discretizes the system's equations of motion using the linear normal modes, and then applies the theory developed for non-linear discrete systems (see [5, 7, 8]). The first approach will hereafter be referred to as the "continuous non-linear normal mode method", whereas the second one will be referred to as the "discretized non-linear normal mode method".

Section 3 contains a complete study of the application of both non-linear normal mode methods to a linear continuous system with a discrete non-linearity, namely, a simply supported Euler–Bernoulli beam constrained by a purely cubic spring . (See [7] for an example with both

quadratic and cubic non-linearities.) For this example, a comparison of both methods as regards accuracy and reliability is held in Section 3.3, which demonstrates that the "continuous" approach is less reliable. Standard projection of the partial differential equation (PDE) of motion onto the linear modes, followed by direct integration of the system of coupled non-linear equations thus obtained (e.g., using a fourth-order Runge–Kutta scheme) are also performed, and several motion simulations are carried out for all methods, so as to obtain *quantitative* comparisons of the performance of the "invariant manifold" approach versus that of the classical modal analysis technique for a continuous system. The invariance properties of the non-linear manifolds under a purely non-linear modal motion are clearly demonstrated by the simulations. It is also shown in Section 3.4 that a purely non-linear modal motion may require many linear modes (i.e., many coupled non-linear equations) to obtain a level of accuracy that can be achieved by only *one* non-linear equation (by definition of a non-linear mode) when using the invariant manifold formulation. For example, two widely used methods – the linearization of the equations of motion, and the projection of them onto a single linear mode (the one that is tangent to the non-linear normal mode manifold considered at the equilibrium point) are shown to yield very poor and moderately good results only, respectively, at costs comparable to that of the non-linear manifold approach. Evidently, such results only apply to non-linear normal mode motions of the particular system studied here, but they do reveal the suspected potential the invariant manifold approach holds in the formulation of a non-linear modal analysis methodology. It is expected that significant savings could be also achieved for general motions of weakly non-linear systems.

2. Normal Modes for Non-Linear Continuous Systems: A Brief Review

The methods developed in [5–8] are quite simple in concept: determine a set of two-dimensional invariant manifolds in the system's phase space which represents normal mode motions for the non-linear oscillatory system, and then derive the equations of motion which dictate the dynamics on the manifolds. Utilizing the existence of the linear normal modes of the linearized system, one can theoretically construct locally, for weakly non-linear systems, formal asymptotic series expansions to any order for these non-linear normal mode manifolds and the attendant modal oscillators. These series systematically contain the non-linear corrections to the linear normal modes of the system, and exactly recover the linear dynamics when non-linearities are neglected.

2.1. Continuous Non-Linear Normal Mode Method

The definition of non-linear normal modes of vibration for one-dimensional continuous systems is directly issued from the theory elaborated in [5] for discrete systems. Namely, *a normal mode of motion for a non-linear, autonomous oscillatory system is a motion which takes place on a two-dimensional invariant manifold in the system's phase space. This manifold passes through a stable equilibrium point of the system, and it is tangent to an eigenspace of the system linearized about that equilibrium.*

Therefore, an invariant manifold, and the dynamics of the system on it, can be described by a pair of independent coordinates. These can be chosen to be the displacement $u_0(t)$ and the velocity $v_0(t)$ of a particular point $s = s_0$ of the structure, as shown in Figure 1 (u_0 and

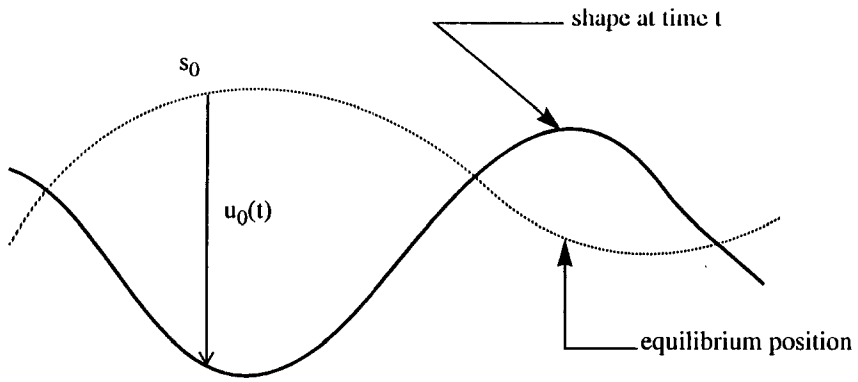

Fig. 1. Generic one-dimensional continuous system.

v_0 are considered independent). The displacement and velocity fields of the entire system for a normal mode motion are then formulated as

$$\begin{cases} u(s,t) = U(u_0(t), v_0(t), s, s_0) \\ v(s,t) = V(u_0(t), v_0(t), s, s_0) \end{cases} \tag{1}$$

which describes a two-dimensional manifold in the infinite-dimensional phase space of the system.

The equations of motion of the continuous system are assumed to be in first-order form as follows

$$\begin{cases} \dfrac{\partial u(s,t)}{\partial t} = v(s,t) \\ \\ \dfrac{\partial v(s,t)}{\partial t} = F(u(s,t), v(s,t)) \end{cases} \quad \text{for } s \in \Omega - \partial\Omega, \tag{2}$$

where F is a non-linear differential operator (note that obtaining F may require the inversion of an inertia-operator), Ω is the domain of s, and $\partial\Omega$ is its boundary, with the boundary conditions

$$B(u(s,t), v(s,t)) = 0 \quad s \in \partial\Omega. \tag{3}$$

The geometric constraints, equation (1), can be used to eliminate the explicit time dependence in equation (2), hence yielding a set of equations which describes the geometry of the system's invariant manifolds. Once the geometry of these invariant manifolds is known (usually in a local sense, by means of a series expansion), i.e., once the functions U and V are solved for for each mode, the dynamics on each of them are easily obtained by first evaluating the equations of motion, equation (2), at the point $s = s_0$ (to determine $u_0(t)$ and $v_0(t)$), and then using the constraint equations, equation (1), to obtain the dynamics of any other point. The first step of this procedure yields a second-order non-linear oscillator equation describing the dynamics of the system undergoing a purely single non-linear mode motion, and allows for the derivation of some physical characteristics of the dynamics of this motion, such as the amplitude-dependent frequency or the amplitude decay rate. This methodology is fully explained in [6], and it is applied to the example considered in this paper hereafter.

Note that this method is outlined here for one-dimensional systems under the assumption that all manifolds are two-dimensional, which implies simple, non-resonant eigenvalues and

underdamped modes for the linearized system. It can however be generalized to handle the cases of overdamped systems or of multiply repeated frequencies for multi-dimensional systems. It is also important to notice that the method can theoretically handle many types of forces, including dissipative, and other non-conservative or gyroscopic forces, as long as they are sufficiently smooth. Note also that when linear systems are considered, this approach is completely equivalent to the traditional eigenvalue problem, in the sense that the eigensolutions (i.e., the normal modes) are exactly recovered, although it does so in a novel manner [6].

2.2. Discretized Non-Linear Normal Mode Method

An alternative and perhaps more practical methodology to determine the non-linear normal modes of a continuous system is one that is based on the prior Galerkin-type discretization of the partial differential equation governing the system, and the subsequent normal mode calculation for the non-linear discretized system. This approach has very recently been introduced in [8] for systems with cubic non-linearities, and extended to systems with quadratic and cubic non-linearities in [7].

The equations of motion are assumed to be of the form

$$M\left[\frac{\partial^2 u}{\partial t^2}(s,t)\right] + L[u(s,t)] + N[u(s,t)] = 0, \quad s \in \Omega - \partial\Omega, \tag{4}$$

with the boundary conditions

$$B(u(s,t), v(s,t)) = 0, \quad s \in \partial\Omega, \tag{5}$$

where L and M are the linear, self-adjoint, positive definite stiffness and mass differential operators(so that the linearized system undergoes oscillatory motions), respectively, and N is a non-linear differential operator. One can decompose the exact solution onto the normal modes of the linearized system, as

$$u(s,t) = \sum_{j=1}^{\infty} \phi_j(s)\eta_j(t) \tag{6}$$

where the η_j's are the linear modal coordinates corresponding to the linear mode shapes ϕ_j, $j = 1, \ldots, \infty$.

Projecting the equations of motion onto the linear modes then yields

$$\sum_{j=1}^{\infty} \langle \phi_i, M(\phi_j)\rangle \ddot{\eta}_j + \sum_{j=1}^{\infty} \langle \phi_i, L(\phi_j)\rangle \eta_j + \left\langle \phi_i, N\left(\sum_{j=1}^{\infty} \phi_j \eta_j\right)\right\rangle = 0, \quad i = 1, \ldots, \infty \tag{7}$$

where $\langle f, g\rangle$ denotes the usual inner product defined as $\langle f, g\rangle = \int_\Omega f(s)g(s)\,\mathrm{d}s$.

For the linearized system, the mode shapes satisfy

$$\langle \phi_i, M(\phi_j)\rangle = \mu_i \delta_{ij} \tag{8}$$

$$\langle \phi_i, L(\phi_j)\rangle = \mu_i \omega_i^2 \delta_{ij} \tag{9}$$

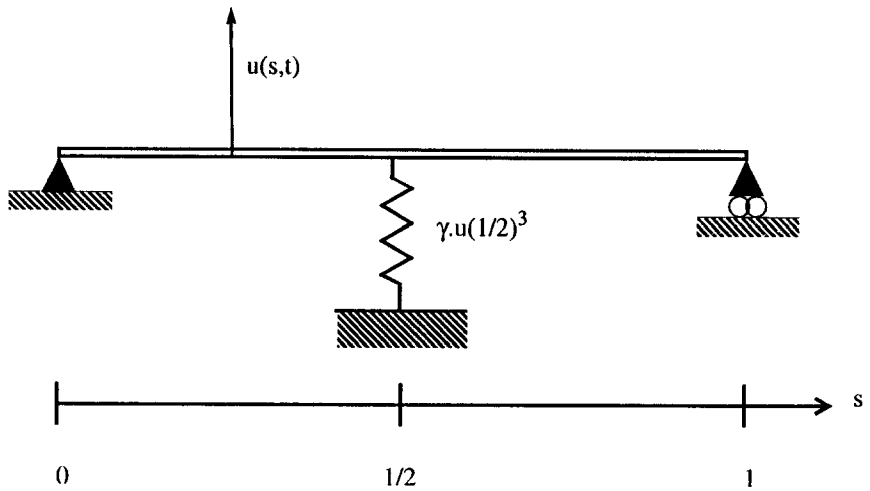

Fig. 2. Simply-supported Euler–Bernoulli (linear) beam connected to a purely cubic spring.

where δ_{ij} is the Kronecker delta and μ_i is the modal mass, so that equation (7) becomes a set of non-linear ordinary differential equations (ODEs) decoupled at the linear order but coupled via non-linear terms:

$$\ddot{\eta}_i + \omega_i^2 \eta_i + N_i(\underset{\sim}{\eta}) = 0, \quad i = 1, \ldots, \infty \tag{10}$$

where $\ddot{\eta}_i = \partial^2 \eta_i / \partial t^2$, $\underset{\sim}{\eta}$ is the vector of all the linear modal coordinates, and $N_i(\underset{\sim}{\eta}) = 1/\mu_i \langle \phi_i, N(\sum_{j=1}^{\infty} \phi_j \eta_j) \rangle$, $i = 1, \ldots, \infty$.

The theory developed in [5] for discrete systems can then be applied to this set of non-linear ODEs, which allows for the definition of the non-linear normal modes of vibration of a discrete system as two-dimensional invariant manifolds tangent to the modes of the linearized system near the equilibrium point of interest. For that purpose, one must define a pair of independent coordinates for each mode, so as to describe the invariant manifolds (at least in a local sense).

Note that both the "continuous" and the "discretized" non-linear normal mode methods are consistent and theoretically yield equivalent non-linear normal modes for continuous systems. Also note that, while the "continuous" non-linear normal mode approach is primarily defined for one-dimensional systems and necessitates generalization for two- and three-dimensional systems, the "discretized" non-linear normal mode approach is directly appropriate for systems of any dimensions, since the partial differential equations of motion are discretized using the modes of the multi-dimensional linearized system.

3. Non-Linear Normal Modes, Invariance, and Comparison of Modal Dynamics Approximations on a Study Case

3.1. Equation of Motion for a Linear Beam Constrained by a Purely Non-Linear Spring

The system chosen to implement the above methods and explore and compare their utility and performance is a homogeneous, simply supported Euler–Bernoulli beam with a non-linear cubic spring attached at its middle – see Figure 2. While the beam itself is assumed to deform

in the linear range, the spring was chosen as purely cubic so that the linearized system's normal modes were those of the simply supported beam alone (i.e., pure sine waves), and therefore so that the influence of the various linear modes on the non-linear ones could be visualized easily. Notice that, since the spring is located at a node of the antisymmetric (even) modes, it will not affect them, so that the antisymmetric modes of the non-linear system will be the same as those of the linearized system. Therefore, only the symmetric (odd) modes will be influenced by the non-linear spring and, furthermore, they will only feature contributions of the symmetric linear modes.

If the beam is of length $l = 1$, the equation of transverse motion can be shown to be

$$m\ddot{u} + EIu_{,ssss} + \gamma u^3 \delta\left(s - \frac{1}{2}\right) = 0, \quad s \in]0, 1[\tag{11}$$

or in non-dimensional form:

$$\ddot{u} + \alpha u_{,ssss} + \beta u^3 \delta\left(s - \frac{1}{2}\right) = 0, \quad s \in]0, 1[\tag{12}$$

where E is Young's modulus for the beam, I is the second moment of area for the cross-section, m is its mass per unit length, γ is the non-linear stiffness of the spring, s represents the spatial coordinate along the beam, $u(s, t)$ is the transverse deflection, $(.)_{,s}$ denotes a derivative with respect to s, an overdot represents a derivative with respect to time, $\delta(.)$ is the Dirac function, $\alpha = EI/m$ and $\beta = \gamma/m$.

The associated boundary conditions are

$$\begin{cases} u(0) = 0 \\ u(1) = 0 \end{cases} \quad \text{and} \quad \begin{cases} u_{,ss}(0) = 0 \\ u_{,ss}(1) = 0. \end{cases} \tag{13}$$

3.2. Non-Linear Normal Modes

3.2.1. *Continuous Non-Linear Normal Mode Method*

The method is described fully in [6]. Since for this example, most of the derivation of the normal modes is fairly straightforward, only the essential steps are given here.

The equation of motion is first written in first-order form as:

$$\begin{cases} \dfrac{\partial u}{\partial t} = v \\ \dfrac{\partial v}{\partial t} = -\alpha u_{,ssss} - \beta u^3 \delta\left(s - \dfrac{1}{2}\right). \end{cases} \tag{14}$$

In order to seek non-linear normal mode motions, the displacement and velocity of any point on the beam are functionally related to the displacement and velocity of an arbitrary point $s = s_0$ as follows

$$\begin{cases} u(s, t) = U(u_0(t), v_0(t), s, s_0) \\ v(s, t) = V(u_0(t), v_0(t), s, s_0) \end{cases} \tag{15}$$

where $u_0(t) = u(s_0, t)$ and $v_0(t) = \mathrm{d}/\mathrm{d}t(u_0) = v(s_0, t)$. The time-derivatives of u and v on the modal manifold are obtained as follows

$$\begin{cases} \dfrac{\partial u}{\partial t} = \dfrac{\partial U}{\partial u_0} \times \dot{u}_0 + \dfrac{\partial U}{\partial v_0} \times \dot{v}_0 \\ \dfrac{\partial v}{\partial t} = \dfrac{\partial V}{\partial u_0} \times \dot{u}_0 + \dfrac{\partial V}{\partial v_0} \times \dot{v}_0 \end{cases} \tag{16}$$

with

$$\begin{cases} \dot{u}_0 = v_0 \\ \dot{v}_0 = -\alpha \dfrac{\partial^4 U}{\partial s^4}(s_0, t) - \beta u_0^3 \delta\left(s_0 - \dfrac{1}{2}\right). \end{cases} \tag{17}$$

Substitution of equations (16) and (17) into equation (14) results into a set of constraint equations for the geometry of the manifolds, in which the explicit time dependence of the problem has been removed:

$$\begin{cases} V = \dfrac{\partial U}{\partial u_0} \times v_0 + \dfrac{\partial U}{\partial v_0}\left[-\alpha \dfrac{\partial^4 U}{\partial s^4}(s_0, t) - \beta u_0^3 \delta\left(s_0 - \dfrac{1}{2}\right)\right] \\ -\alpha \dfrac{\partial^4 U}{\partial s^4} - \beta U^3 \delta\left(s - \dfrac{1}{2}\right) \\ \qquad = \dfrac{\partial V}{\partial u_0} \times v_0 + \dfrac{\partial V}{\partial v_0}\left[-\alpha \dfrac{\partial^4 U}{\partial s^4}(s_0, t) - \beta u_0^3 \delta\left(s_0 - \dfrac{1}{2}\right)\right]. \end{cases} \tag{18}$$

Notice that so far, no assumption has been made on U and V, and therefore equation (18) describes the non-linear normal mode in a non-local sense, that is, if one can find the exact solution of equation (18), this solution will describe the exact shape of the manifold. However, this is in general not possible.

For the system considered here, the exact solutions (i.e., the solution for each non-linear normal mode) to equation (18) could not be found explicitly (except for the even modes, which are not affected by the non-linearity). However, the local characteristics of the invariant manifold geometry (and also of the dynamics on them) can be determined by expanding U and V in Taylor series with respect to u_0 and v_0. To third order, this yields, for the ith non-linear mode:

$$\begin{cases} U_i = a_1^i u_0 + a_2^i v_0 + a_3^i u_0^2 + a_4^i u_0 v_0 + a_5^i v_0^2 + a_6^i u_0^3 \\ \qquad + a_7^i u_0^2 v_0 + a_8^i u_0 v_0^2 + a_9^i v_0^3 + \cdots \\ V_i = b_1^i u_0 + b_2^i v_0 + b_3^i u_0^2 + b_4^i u_0 v_0 + b_5^i v_0^2 + b_6^i u_0^3 \\ \qquad + b_7^i u_0^2 v_0 + b_8^i u_0 v_0^2 + b_9^i v_0^3 + \cdots \end{cases}, \tag{19}$$

where the a_j^i's and the b_j^i's are functions of the space variable s.

Substituting equation (19) into equation (18) and equating the coefficients of like powers in u_0 and v_0 yields a set of differential equations which have to be solved for the a_j^i's and the b_j^i's, subject to the set of boundary conditions

$$\begin{cases} a_j^i(0) = 0 \\ a_j^i(1) = 0 \\ (a_j^i)''(0) = 0 \\ (a_j^i)''(1) = 0 \end{cases} \qquad \begin{cases} b_j^i(0) = 0 \\ b_j^i(1) = 0 \\ (b_j^i)''(0) = 0 \\ (b_j^i)''(1) = 0. \end{cases} \tag{20}$$

Note that the following equalities must hold at s_0:

$$\begin{cases} a_1^i(s_0) = 1 \\ b_2^i(s_0) = 1 \end{cases} \qquad \begin{cases} a_j^i(s_0) = 0, \ j \neq 1 \\ b_j^i(s_0) = 0, \ j \neq 2. \end{cases} \tag{21}$$

Solving these boundary value problems in the a_j^i's and b_j^i's is a fairly tedious but not complicated process. Besides, the calculations for the present example are similar to those for a beam on a non-linear elastic foundation, which was solved for in full detail in [6]. Therefore, only the results and the main features of their derivation are given here.

Considering the ith non-linear mode, one first solves for the terms at the linear order, which are readily found to be

$$a_1^i(s) = b_2^i(s) = \frac{\sin(i\pi s)}{\sin(i\pi s_0)}, \quad i = 1, \ldots, N \tag{22}$$

$$a_2^i(s) = b_1^i(s) = 0. \tag{23}$$

Notice that up to the linear order, the normal modes of the linearized system are recovered – with a particular scaling – which is a direct consequence of the definition itself of the non-linear normal modes (which are tangent to their linear counterpart at the system's equilibrium point). Also note that equation (22) precludes s_0 to be a node for the ith mode of the linearized system, i.e., we must have $\sin(i\pi s_0) \neq 0$.

The set of differential equations to be solved for the quadratic coefficients is linear and homogeneous with homogeneous boundary conditions, and its solutions are zero, as they ought to be in the absence of quadratic non-linearities. The equations for the cubic coefficients a_7^i, a_9^i, b_6^i and b_8^i are uncoupled from those involving the cubic coefficients a_6^i, a_8^i, b_7^i and b_9^i, and are homogeneous, implying that their solutions are also zero.

The coefficients b_7^i and b_9^i are easily eliminated from the remaining four equations, resulting in a boundary value problem to be solved for the cubic coefficients a_6^i and a_8^i, given by

$$\alpha a_6^{i\prime\prime\prime\prime} - 3\alpha(i\pi)^4 a_6^i + 2\alpha^2(i\pi)^8 a_8^i = \alpha a_6^{i\prime\prime\prime\prime}(s_0)\frac{\sin(i\pi s)}{\sin(i\pi s_0)} - \beta\left[\frac{\sin(i\pi s)}{\sin(i\pi s_0)}\right]^3 \delta\left(s - \frac{1}{2}\right) \tag{24}$$

$$\alpha a_8^{i\prime\prime\prime\prime} - 7\alpha(i\pi)^4 a_8^i + 6a_6^i = \alpha a_8^{i\prime\prime\prime\prime}(s_0)\frac{\sin(i\pi s)}{\sin(i\pi s_0)} \tag{25}$$

for $s_0 \neq 1/2$ (for singularity reasons) and $\sin(i\pi s_0) \neq 0$, with the corresponding homogeneous boundary conditions given in equations (20) and (21).

In order to solve accurately for the cubic coefficients, one has to perform first a change of unknown functions in order to improve the smoothness of the solutions. This is because the solutions of equations (24) and (25) are only twice continuously differentiable, due to the occurrence of the Dirac function in the non-homogeneous term in equation (24). Since these solutions will be sought in the form of infinitely differentiable series, this change of functions will improve the convergence of the series solution. This is achieved by defining $\bar{a}_6^i(s)$ as

$$\bar{a}_6^i(s) = a_6^i(s) + F_i(s) \tag{26}$$

while keeping $a_8^i(s)$ unchanged. The function $F_i(s)$ is chosen so that it carries the discontinuity of the higher derivatives, but does not perturb the boundary conditions, that is:

$$\begin{cases} F_i(0) = F_i(1) = 0 \\ F_i''(0) = F_i''(1) = 0 \end{cases} \tag{27}$$

and

$$F_i''''(s) = \frac{\beta}{\alpha}\left[\frac{\sin(i\pi s)}{\sin(i\pi s_0)}\right]^3 \delta\left(s - \frac{1}{2}\right). \tag{28}$$

Integrating equation (28) while enforcing continuity of F_i and of its first and second derivatives yields:

$$F_i(s) = \frac{\beta}{\alpha}\left[\frac{\sin(i\frac{\pi}{2})}{\sin(i\pi s_0)}\right]^3 \times \begin{cases} -\dfrac{s}{12}\left[s^2 - \dfrac{3}{4}\right] & \text{for } 0 \le s < 1/2 \\ \dfrac{(s-1)}{12}\left[(s-1)^2 - \dfrac{3}{4}\right] & \text{for } 1/2 < s \le 1. \end{cases} \tag{29}$$

Carrying out the change of functions, equation (26), into equations (24) and (25) yields a new set of differential equations (valid for $s_0 \neq 1/2$ and $\sin(i\pi s_0) \neq 0$) in terms of $\bar{a}_6^i$ and a_8^i, which are now six times continuously differentiable functions:

$$\begin{cases} \bar{a}_6^{i\prime\prime\prime\prime} - 3(i\pi)^4 \bar{a}_6^i + 2\alpha(i\pi)^8 a_8^i = \bar{a}_6^{i\prime\prime\prime\prime}(s_0)\dfrac{\sin(i\pi s)}{\sin(i\pi s_0)} - 3(i\pi)^4 F_i(s) \\ \alpha a_8^{i\prime\prime\prime\prime} - 7\alpha(i\pi)^4 a_8^i + 6\bar{a}_6^i = \alpha a_8^{i\prime\prime\prime\prime}(s_0)\dfrac{\sin(i\pi s)}{\sin(i\pi s_0)} + 6F_i(s) \end{cases} \tag{30}$$

with boundary conditions immediately following from equations (20), (26) and (27). The process can of course be iterated several times if needed, to achieve further smoothness of the solution. Equation (30) would be fairly complicated to solve exactly, but approximate solutions can be found by expanding $\bar{a}_6^i$, a_8^i and F_i into the modes of the linearized system, that is:

$$\bar{a}_6^i = \sum_{j=1}^{\infty} \alpha_j^i \sin(j\pi s) \tag{31}$$

$$a_8^i = \sum_{j=1}^{\infty} \beta_j^i \sin(j\pi s) \tag{32}$$

$$F_i = \sum_{j=1}^{\infty} f_j^i \sin(j\pi s). \tag{33}$$

The resulting system of equations for the α_j^i's and the β_j^i's is linear in the unknowns and can be solved easily. Those coefficients are

$$\begin{cases} \alpha_j^i = \dfrac{-3(i\pi)^4[(j\pi)^4 - 7(i\pi)^4] - 12(i\pi)^8}{[(j\pi)^4 - 7(i\pi)^4][(j\pi)^4 - 3(i\pi)^4] - 12(i\pi)^8} \times f_j^i \\ \beta_j^i = \dfrac{6(j\pi)^4}{\alpha[[(j\pi)^4 - 7(i\pi)^4][(j\pi)^4 - 3(i\pi)^4] - 12(i\pi)^8]} \times f_j^i \end{cases} \quad \text{for } j \neq i \tag{34}$$

where

$$f_j^i = 2\beta \left[\frac{\sin(i\frac{\pi}{2})}{\sin(i\pi s_0)}\right]^3 \frac{\sin(j\frac{\pi}{2})}{(j\pi)^4} \tag{35}$$

and

$$\alpha_i^i = f_i^i - \frac{1}{9(i\pi)^4} \frac{1}{\sin(i\pi s_0)} \sum_{\substack{j=1 \\ j\neq i}}^{\infty} [7\alpha_j^i + 2\alpha(i\pi)^4 \beta_j^i](j\pi)^4 \sin(j\pi s_0) \tag{36}$$

$$\beta_i^i = -\frac{1}{3\alpha(i\pi)^8} \frac{1}{\sin(i\pi s_0)} \sum_{\substack{j=1 \\ j\neq i}}^{\infty} [2\alpha_j^i + \alpha(i\pi)^4 \beta_j^i](j\pi)^4 \sin(j\pi s_0). \tag{37}$$

The cubic coefficients $a_6^i(s)$ and $a_8^i(s)$ are then recovered by equations (31), (32) and (26), while the coefficients $b_7^i(s)$ and $b_9^i(s)$ are given by

$$\begin{cases} b_7^i(s) = 3a_6^i(s) - 2(i\pi)^4 a_8^i(s) \\ b_9^i(s) = a_8^i(s) \end{cases} \tag{38}$$

The ith non-linear normal mode is then determined up to third order by

$$\begin{cases} U_i = a_1^i(s)u_0 + a_6^i(s)u_0^3 + a_8^i(s)u_0 v_0^2 + \cdots \\ V_i = b_2^i(s)v_0 + b_7^i(s)u_0^2 v_0 + b_9^i(s)v_0^3 + \cdots \end{cases} \tag{39}$$

with the coefficients found above.

Note that whenever $u_0 = 0$, (i.e., when the displacement at the chosen point s_0 is zero), then $u(s,t) = 0$ for all s at that instant of time. Likewise, when $v_0 = 0$, then $v(s,t) = 0$ for all s, i.e., $u(s,t)$ is extremum for all s. Consequently, the beam motion in a given non-linear normal mode is synchronous, since all points have zero deflection and reach their maximum amplitude at the same times. (For cases with both quadratic and cubic non-linearities, the motion is no longer synchronous and various points would not necessarily have zero deflection at the same time. They would however reach their maximum amplitude simultaneously (see [7]).) As in the linear case, the mode shape can then be plotted at any instant of time, in particular when $v_0 = 0$. Notice, however, that the non-linear normal mode shapes are amplitude dependent.

The maximum deflection shape for $v_0 = 0$ depends non-linearly on the maximum amplitude, $u_{0\max}$, as follows:

$$u^i_{\max}(s) = a^i_1(s)u_{0\max} + a^i_6(s)u^3_{0\max} + \cdots \tag{40}$$

where, from this point on, the superscript on $u^i(s,t)$ (respectively, on $u^i_{\max}(s)$) refers to the deflection of the point of abscissa s at time t (respectively, to the maximum deflection of the point of abscissa s) when the system undergoes a motion in the ith non-linear normal mode.

At this point, the dynamics of the ith non-linear mode for the special point s_0 can be obtained by substituting equation (39) into the equation of motion, equation (12), and evaluating the result at $s = s_0$ (where $s_0 \neq 1/2$ and $\sin(i\pi s_0) \neq 0$), yielding

$$\ddot{u}_0 + \alpha[a^{i\prime\prime\prime\prime}_1(s_0)u_0 + a^{i\prime\prime\prime\prime}_6(s_0)u^3_0 + a^{i\prime\prime\prime\prime}_8(s_0)u_0\dot{u}^2_0] + \cdots = 0.$$

The dynamics at any other point follows from equation (39).

3.2.2. *Discretized Non-Linear Normal Mode Method*

Here the beam deflection, $u(s,t)$, is first decomposed onto a subset of the normal modes of the linearized system, ϕ_j, using a standard Galerkin procedure:

$$u(s,t) \simeq \sum_{j=1}^{N} \eta_j(t)\phi_j(s) \tag{41}$$

where N is the number of terms retained in the Galerkin expansion. Given that for the system in Figure 2, the constraining spring is purely non-linear, the linearized system reduces to a classical simply supported Euler–Bernoulli beam, whose linear modes are the well-known $\phi_j(s) = \sin(j\pi s)$. Substituting the Galerkin expansion, equation (41), into the equation of motion (12) and projecting onto the ith linear mode, one obtains

$$\ddot{\eta}_i + \alpha(i\pi)^4\eta_i + 2\beta\left[\sum_{j=1}^{N}\eta_j \sin\left(j\frac{\pi}{2}\right)\right]^3 \sin\left(i\frac{\pi}{2}\right) = 0, \quad i = 1,\ldots,N. \tag{42}$$

This set of N, coupled, non-linear ODEs describes the dynamics of the linear modal components of the motion. These equations can be numerically integrated (e.g., using a fourth-order accurate Runge–Kutta time-marching scheme) to obtain what can be considered (if N is large enough) as the "exact" dynamics of the system. It should be realized at this point that this may be computationally very demanding, since the more accurate the desired solution, the larger the number of coupled ODEs to be solved (recall that for a Runge–Kutta scheme, the actual number of first-order equations is $2N$).

One can also obtain approximations of the non-linear normal modes of the system by applying to this set of N non-linear ODEs the general method developed in [5]. In order to do so, one has first to express the problem into a set of $2N$ first-order ODEs, as

$$\begin{cases} \dot{x}_i = y_i \\ \dot{y}_i = f_i(x_1,\ldots,x_N,y_1,\ldots,y_N) \end{cases} \quad i = 1,\ldots,N \tag{43}$$

where $x_i = \eta_i$, $y_i = \dot{\eta}_i$, and

$$f_i = -\alpha(i\pi)^4 x_i - 2\beta \left[\sum_{j=1}^{N} x_j \sin\left(j\frac{\pi}{2}\right)\right]^3 \sin\left(i\frac{\pi}{2}\right). \tag{44}$$

Then, a pair of independent coordinates, (u_k, v_k), must be chosen to describe the geometry of the invariant manifold for each non-linear normal mode. It is here a natural choice to define

$$\begin{cases} u_k = x_k = \eta_k \\ v_k = y_k = \dot{\eta}_k \end{cases} \tag{45}$$

for the kth non-linear mode. The x_i's and y_i's (for $i \neq k$) are then assumed to be functionally related to u_k and v_k as

$$\begin{cases} x_i = X_i(u_k, v_k) \\ y_i = Y_i(u_k, v_k) \end{cases} \quad i = 1, \ldots, N, \quad i \neq k\,. \tag{46}$$

Taking the time-derivative of equation (46) yields:

$$\begin{cases} \dot{X}_i = \dfrac{\partial X_i}{\partial u} \times \dot{u}_k + \dfrac{\partial X_i}{\partial v} \times \dot{v}_k \\ \dot{Y}_i = \dfrac{\partial Y_i}{\partial u} \times \dot{u}_k + \dfrac{\partial Y_i}{\partial v} \times \dot{v}_k \end{cases} \quad i = 1, \ldots, N, \quad i \neq k. \tag{47}$$

Note that one can define $X_k(u_k, v_k) = u_k$ and $Y_k(u_k, v_k) = v_k$ for consistency of notation in the derivations.

Substituting equations (46) and (47) into equation (42), the equations governing the geometry of the invariant manifold of the kth non-linear normal mode are:

$$\begin{cases} Y_i = \dfrac{\partial X_i}{\partial u} \times v_k + \dfrac{\partial X_i}{\partial v} \times f_k \\ f_i = \dfrac{\partial Y_i}{\partial u} \times v_k + \dfrac{\partial Y_i}{\partial v} \times f_k \end{cases} \quad i = 1, \ldots, N, \quad i \neq k \tag{48}$$

which are to be solved for the X_i's and Y_i's.

An approximate local solution can be computed by assuming a Taylor series expansion of X_i and Y_i with respect to u_k and v_k up to the desired order. In this case, because of the purely cubic non-linearity in the equation of motion and its conservative, non-gyroscopic nature, many terms are zero and the Taylor series expansions reduce to, up to third order:

$$\begin{cases} X_i = a_1^i u_k + a_6^i u_k^3 + a_8^i u_k v_k^2 + \cdots \\ Y_i = b_2^i v_k + b_7^i u_k^2 v_k + b_9^i v_k^3 + \cdots \end{cases} \quad i = 1, \ldots, N, \quad i \neq k. \tag{49}$$

Substituting equation (49) into equation (48) and equating the coefficients of like powers in u_k and v_k, one obtains:

(1) *if k is even*:

$$a_6^i = a_8^i = 0, \quad i = 1, \ldots, N, \quad i \neq k$$

(2) *if k is odd*:

– if i is even:

$$a_6^i = a_8^i = 0, \quad i = 1, \ldots, N, \quad i \neq k$$

– if i is odd:

$$a_6^i = 2\beta(-1)^{(k+i/2)} \frac{[i^4 - 7k^4]}{\alpha\pi^4[i^4 - k^4][i^4 - 9k^4]}, \quad i = 1, \ldots, N, \quad i \neq k \tag{50}$$

$$a_8^i = -12\beta(-1)^{(k+i/2)} \frac{1}{\alpha^2\pi^8[i^4 - k^4][i^4 - 9k^4]}, \quad i = 1, \ldots, N, \quad i \neq k \tag{51}$$

and, for all k and $i = 1, \ldots, N$, $i \neq k$:

$$\begin{cases} b_2^i = a_1^i = 0 & \text{and } b_2^k = a_1^k = 1, \\ b_7^i = -2\alpha\pi^4 k^4 a_8^i + 3a_6^i \\ b_9^i = a_8^i. \end{cases} \tag{52}$$

The coefficients a_6^i and a_8^i represent the non-linear correction in the kth non-linear normal mode due to the ith linear mode. Notice, as stated earlier, that only the symmetric modes are affected by the non-linearity (k odd), and that only the symmetric linear modes contribute to the symmetric non-linear ones (i odd).

The linear modal amplitudes are then recovered as, for the kth non-linear mode (k odd):

$$\begin{cases} \eta_k = u_k \\ \eta_i = 0 & \text{for } i \text{ even } \ i = 1, \ldots, N, \ i \neq k \\ \eta_i = a_6^i u_k^3 + a_8^i u_k v_k^2 + \cdots & \text{for } i \text{ odd } \ i = 1, \ldots, N, \ i \neq k \end{cases} \tag{53}$$

and the kth non-linear normal mode is reconstructed as

$$\begin{aligned} u^k(s,t) &= \sum_{i=1}^{N} \eta_i(t) \sin(i\pi s) \\ &= u_k(t)\sin(k\pi s) + \sum_{\substack{i=1 \\ i \text{ odd}, i \neq k}}^{N} \eta_i(t)\sin(i\pi s) + \cdots \\ u^k(s,t) &= u_k(t)\sin(k\pi s) + \sum_{\substack{i=1 \\ i \text{ odd}, i \neq k}}^{N} [a_6^i u_k^3(t) + a_8^i u_k(t) v_k^2(t)] \sin(i\pi s) + \cdots \end{aligned} \tag{54}$$

where here again, the superscript k in $u^k(s,t)$ refers to the deflection of the point of abscissa s at time t when the system undergoes a motion in the kth non-linear normal mode (not to be confused with $u_k(t)$ which is the non-linear modal coordinate and is not meant to represent the motion of any particular point).

Regarding the synchrony of the motion, the same considerations hold as for the "continuous" non-linear normal mode method, so that the mode shapes can be plotted when $v_k = 0$, that is, when $u_k = u_{k\max}$. The maximum beam deflection is given to third order by

$$u^k_{\max}(s) = u_{k\max}\sin(k\pi s) + \sum_{\substack{i=1\\ i \text{ odd}, i\neq k}}^{N} a^i_6 u^3_{k\max}\sin(i\pi s) + \cdots \tag{55}$$

The dynamics on one particular non-linear mode are obtained by back substitution of equation (53) into equation (42) for $i = k$, determination of the dynamics of $u_k(t)$ (for example by numerical integration), and then by recombination of the beam non-linear modal displacement, $u^k(s,t)$, using equation (54). This process requires solving only one non-linear ODE to determine the motion on each non-linear mode, as compared to the N coupled ODEs involved in a direct integration of equation (42). The result of the substitution of equation (53) into equation (42) for $i = k$ yields

$$\begin{aligned}
&\ddot{u}_k + \alpha(k\pi)^4 u_k + 2\beta\sin^2\left(k\frac{\pi}{2}\right)u_k^3 \\
&\quad + 6\beta u_k^3\left(\sum_{\substack{j=1\\ j \text{ odd}, j\neq k}}^{N}[a^j_6 u_k^2 + a^j_8 \dot{u}_k^2]\sin\left(j\frac{\pi}{2}\right)\right)\sin\left(k\frac{\pi}{2}\right) \\
&\quad + \cdots = 0, \quad k = 1,\ldots,N.
\end{aligned} \tag{56}$$

The modal dynamics of the non-linear system on each two-dimensional invariant manifold are therefore described by a single-degree of freedom non-linear modal oscillator. Note that the dynamics of the N non-linear modal oscillators are decoupled from one another, which accounts for the invariance of the non-linear normal modes.

A very interesting point here is that without any computational effort added to that of computing the third-order correction to the non-linear modes (that is, the a^i_6's and a^i_8's), one can obtain the dynamics on that non-linear mode up to an accuracy of fifth order in a perfectly consistent and legitimate way (see equation (56)), since any correction in the geometry of the invariant manifold of order at least five would yield terms of order at least seven in the dynamics, equation (56). Likewise, the fifth-order approximation of the normal mode geometry would give the dynamics on that mode up to seventh order correctly, and more generally, the accuracy of the dynamics is always two orders of magnitude higher than that of the manifold's geometry itself. This is of course very particular to those systems with only odd non-linearities, but it can be shown easily that even if the system had a quadratic non-linearity, the accuracy of the dynamics on a single non-linear mode would always be one order higher than that of the mode shape.

Note that in our case the application of this result to the first-order non-linear approximation of the normal mode (i.e., the linearized mode) predicts a third order accuracy in the dynamics, which is consistent with the fact that the standard projection of the partial differential equation of motion onto a single linear mode yields the correct frequency correction up to third order.

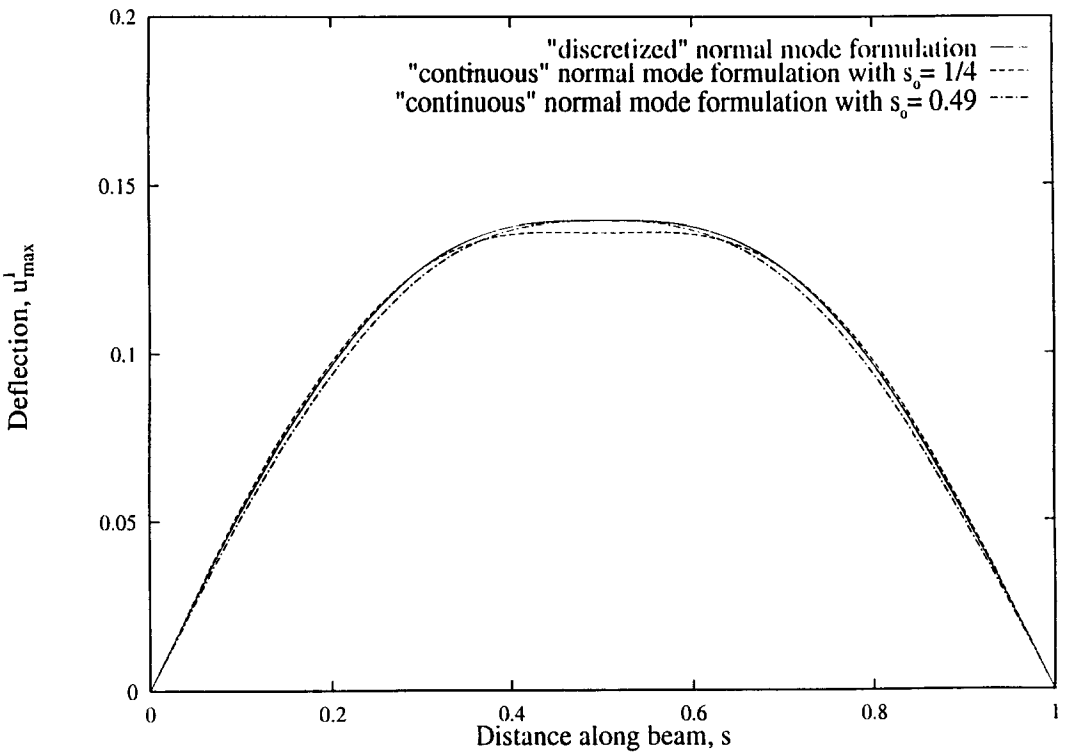

Fig. 3a. Comparison of the first non-linear normal mode shapes obtained by the "discretized" non-linear formulation and the "continuous" non-linear formulation (for two different values of s_0).

3.3. Non-Linear Mode Shapes

Figures 3a and 3b show, respectively, the maximum deflection shapes obtained to third order for the first and third non-linear modes by the two methods presented above, for the values $\alpha = 1$, $\beta = 10^4$, and $u_{k\max} = 0.15$ (u_k being u_1 for the first mode and u_3 for the third mode). For the "continuous" normal mode method, s_0 was chosen first, and u_0 was then determined such that the amplitude at s_0 obtained by both methods matched. Note that in the case where s_0 is close to 1/2, the mode shapes obtained by the two methods agree quite well (s_0 could not be taken at the mid-span exactly since tht was an excluded poin; see Section 3.2.1). However, when s_0 is chosen to be at some other location, the mode shape obtained by the "continuous" normal mode method changes. This has no particular physical meaning and was used in [6] to predict the limit of validity of the method. Moreover, recalling that the method fails when s_0 is taken at a node of a linear mode, it is believed that the dependence of the "continuous" normal mode formulation on s_0 makes it less desirable in general. Indeed, in this example, the method works best (for both the first and third non-linear modes) when s_0 is as far as possible from the nodes (or the end points), i.e., when s_0 is close (but not equal to) $s = 1/2$.

Therefore, the "continuous" non-linear normal mode method, although more appealing in its formulation, was left aside for the remainder of the study. The simulation of the dynamics on the non-linear modes was thus carried out using the Galerkin discretization followed by the discrete non-linear normal mode formulation.

Both methods capture the same qualitative features of the non-linear mode shapes, in which the influence of the various linear modes is evident. In particular, the first non-linear mode

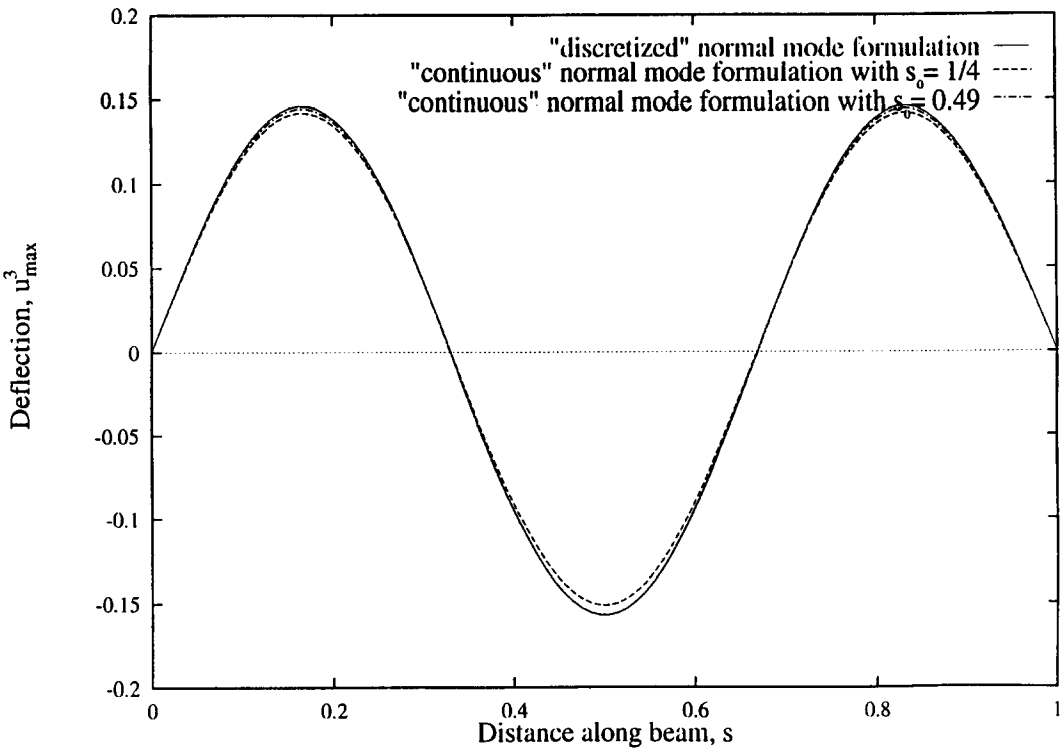

Fig. 3b. Comparison of the third non-linear normal mode shapes obtained by the "discretized" non-linear formulation and the "continuous" non-linear formulation (for two different values of s_0).

depicted in Figure 4a clearly illustrates the influence of the higher linear modes (mainly the third linear mode), indicating that several of them may be needed to recover its dynamics if a standard linear modal analysis of the non-linear system were performed. Figure 4a depicts the growing influence of the higher linear modes on the first non-linear mode shape as the peak amplitude is increased (this was obtained using only the discretized non-linear mode formulation).

In Figure 4b, the influence of the various linear modes on the third non-linear one is evident as well. It is observed that the mode shape is "pulled down" at its middle, a counter-intuitive result. This is mainly due to the contribution of the first linear mode to the third non-linear mode, $a_6^1 \sin(\pi/2)$, which is negative, and therefore acts in the same direction as the coefficient of the third linear mode. Likewise, for any odd non-linear mode, say the kth mode, it can be seen by inspection of $a_6^1 \sin(\pi/2)$ and from the form of the kth linear mode shape that those two components will always act in the same direction. Therefore, for k not too large (so that a_6^1 is still significant), this counter-intuitive phenomenon would be observed as well. Note that it is a fairly easy matter to solve the eigenvalue problem in which a linear spring replaces the non-linear one, and that in that case, the same qualitative mode shape distortions occur. Therefore, it appears that this phenomenon is not due to the non-linear nature of the constraint.

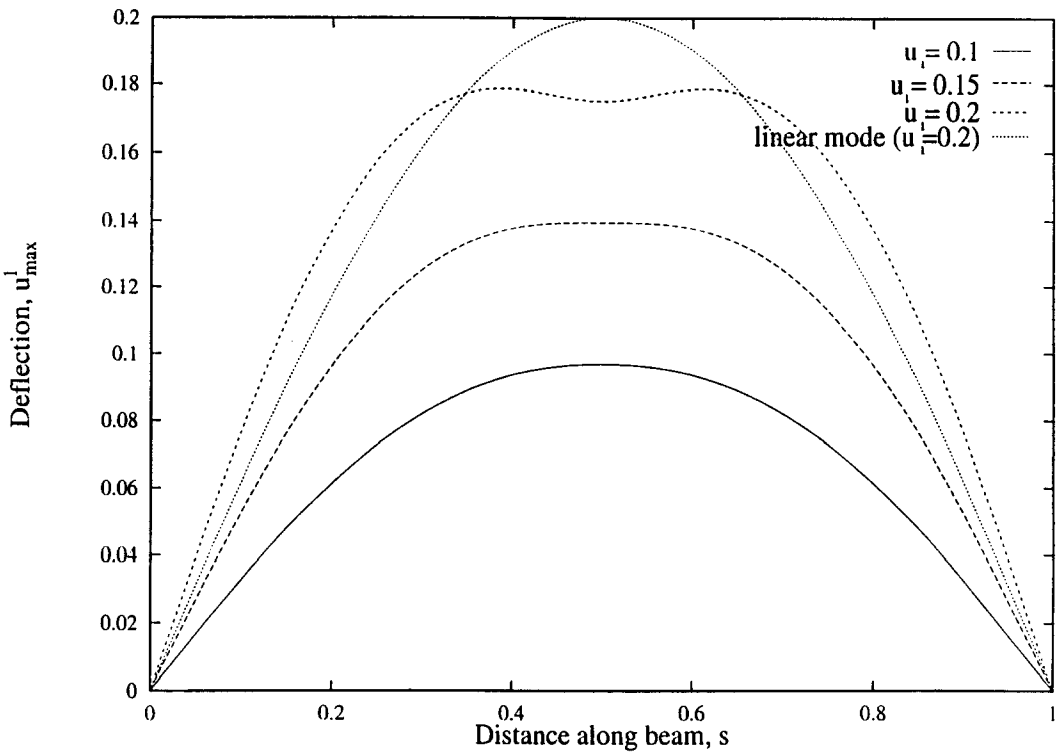

Fig. 4a. The amplitude-dependent shape of the first non-linear normal mode as the amplitude increases (for $\alpha = 1$ and $\beta = 10^4$), using the "discretized" normal mode formulation. The first linear mode shape is shown for $u_1 = 0.2$. Notice the influence of higher (antisymmetric) linear modes.

3.4. Numerical Simulations of the Dynamics on a Non-Linear Normal Mode

Numerical simulations were performed to check the invariance properties of the non-linear normal modes and the accuracy of the series solutions as obtained by the discretized system methodology described in Sections 2.2 and 3.2.2. Another purpose of the simulations was, given the invariance of the non-linear normal modes, to determine how many linear modes were needed to capture the dynamics of the system vibrating in an invariant non-linear normal mode. This gives an indication of the potential pay-off of using non-linear modes in place of linear modes in the analysis of non-linear systems.

Clearly, the higher modes are less affected by the non-linear spring than the lower ones (which can be seen by inspection of the coefficients a^i_6 and a^i_8), and thus the non-linear mode of greatest interest is the first one. It was the one most studied below. Several simulations were carried out, all using a fourth-order Runge–Kutta time-marching scheme (which provided good convergence for all simulations for sufficiently small integration time-steps). Notice that, in practice, in order for the Taylor series expansions of X_i and Y_i to be legitimate for a given non-linear normal mode, u_k and v_k should be of same order of magnitude, which can be obtained by rescaling time as $\tau = \lambda t$. This yields a new set of discretized equations of motion (replacing equation (42)) where α and β are replaced by $\alpha' = \lambda^2\alpha$ and $\beta' = \lambda^2\beta$, respectively (the a^i_j coefficients are modified accordingly). In practice, λ was set as a free coefficient which was determined by trial and error until the simulations showed that u_k and v_k were of the same order of magnitude.

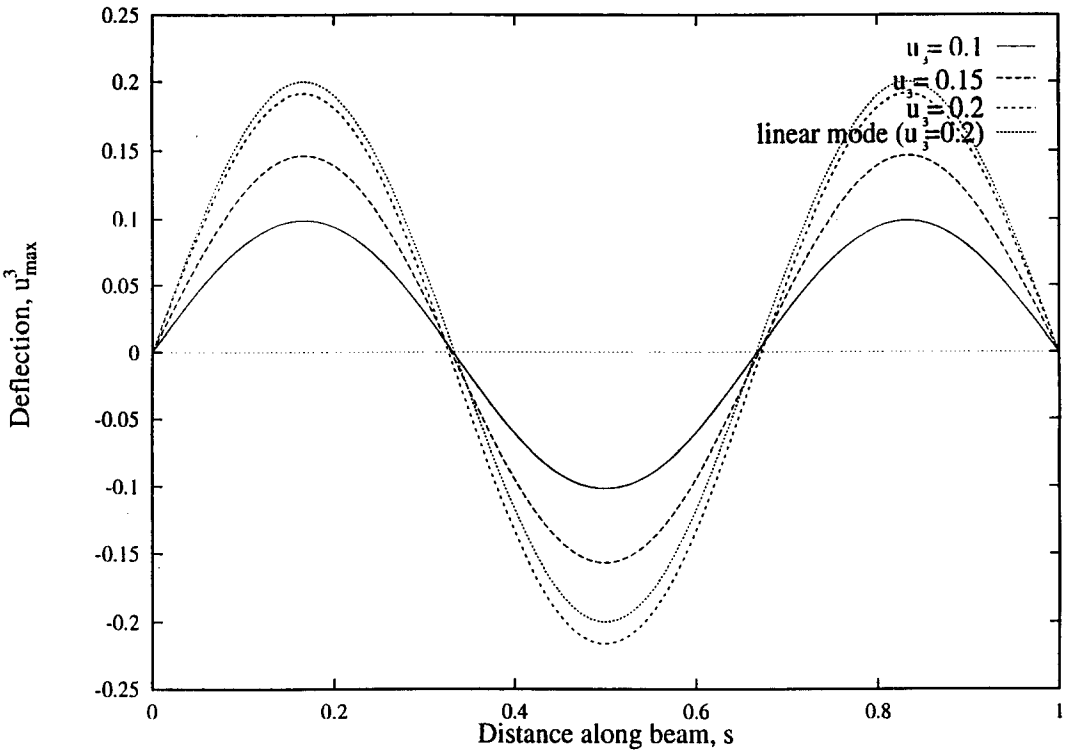

Fig. 4b. The amplitude-dependent shape of the third non-linear normal mode as the amplitude increases (for $\alpha = 1$ and $\beta = 10^4$), using the "discretized" normal mode formulation. The third linear mode shape is shown for $u_3 = 0.2$. The middle-point amplitude is larger in the presence of a spring (non-linear or linear).

The first numerical simulation was the so-called "exact" solution, computed by direct integration of the set of $2N$, non-linear, coupled, first-order ODEs in terms of the linear modal amplitudes and velocities (the rescaled equivalent of equation (42)). If N is large, this theoretically yields a very good approximation of the solution. However, this is computationally expensive, all the more so as the critical time-step for the stability of the scheme is dictated by the Nth pair of first-order equations, which involves frequencies increasing as N^2. This "exact" solution was used to verify the invariance of the motion in a non-linear normal mode and to serve as a reference. Typically, the "exact" solution was calculated with $N = 25$ linear modes, which, in all cases, corresponded to a converged solution (in terms of linear modal coordinates).

The second type of simulations was performed by the non-linear normal mode formulation, but using the dynamics only up to third order (equation (56) up to third order) and then reconstructing the beam motion. The third set of simulations used the full fifth-order dynamics before recombination. The time integrations for these latter two types of simulations were again performed using a fourth-order Runge–Kutta scheme, but only two, first-order, non-linear ODEs in the non-linear modal amplitude and velocity had to be solved for a given non-linear mode in each case. The computational cost was obviously similar in both cases, whereas the results were not. The objective of these two simulations was to validate the non-linear normal mode methodology by verifying the accuracy of the invariance of non-linear normal mode motions.

Other simulations were then carried out from the set of non-linear equations in terms of the linear modal amplitudes and velocities (equation (42), as for the first simulation), in which N was increased from one to five linear modes. Here, the purpose was to study, for a given non-linear mode motion, the modal convergence as the number of linear modes is varied, i.e., to study the influence of the various linear modes on a given non-linear one. Note that an increase of one in N yields two additional non-linear first-order equations, a smaller critical time-step for the stability of the numerical integration, and more complicated non-linear coupling terms. These simulations will be referred to as the linear modal analysis procedure (as opposed to the non-linear normal mode procedure).

Finally, the linearized system, obtained by simple truncation of the higher-order terms in equation (43) was simulated to assess the effect of the non-linearity.

The initial conditions for the various simulations were chosen so that the motion was initiated from a deflection shape which was as close as possible to the first non-linear normal mode shape, with some amplitude and zero velocity. For the linear modal analysis simulations, this was achieved by equating the initial values of the linear modal amplitudes resulting from the Galerkin discretization to the linear mode components of the first non-linear mode shape (equation (55)). Clearly, the larger the number of terms in the Galerkin expansion, the closer the initial deflection shape to the non-linear mode, but the larger the system of non-linear coupled equations, which increases cost. On the other hand, the invariant manifold simulations always require solving only a single pair of ODEs, regardless of how many linear modes are considered in the non-linear mode calculation (equation (55)). Thus, insofar as the non-linear mode shape characteristics are known from previous calculations (namely, the coefficients a_6^i, a_8^i, etc. ...), initiating the motion closer to the invariant manifold only means recombination of more linear components during the simulation to obtain the beam deflection pattern, without a significant increase in computational cost.

The results shown here were obtained with $\alpha = 1$, $\beta = 10^4$ and $u_{k\max} = u_1 = 0.15$, which gave a very significant non-linearity, since the ratio of the non-linear term to the linear one in equation (42) was approximately, for the first mode:

$$\frac{2\beta u_k^3}{\alpha(k\pi)^4 u_k} \sim 4.$$

Simulations were also performed for much smaller non-linearities, and, of course, the smaller the non-linearity, the more accurate were the results obtained using only one or two (odd) linear modes in the linear modal analysis procedure. The results with the larger non-linearity are shown to emphasize the robustness of the theory.

Figure 5 depicts the motion of the mid-point of the beam as obtained by the various simulation schemes. Note that while all of the simulations start with zero initial velocity, which was explicitly imposed, they do not all start with the same initial deflection, due to the different approximations of the non-linear mode shape imposed by the number of linear modes used. It is of course hopeless to expect the correct dynamics on the non-linear mode by starting with as bad an approximation as that given by only one linear mode, although this is a traditional method (in particular to obtain the corresponding frequency correction).

However, it would have been expected that with a large enough number of linear modes, the first non-linear mode would have been somewhat correctly approximated, so as to obtain a periodic motion occurring on the invariant manifold. Figures 5b and 5c show that this is not the case, as observed from the irregular velocities obtained for the "exact" solution. It should be noted at that point that, although this solution does not behave as nicely as expected, there

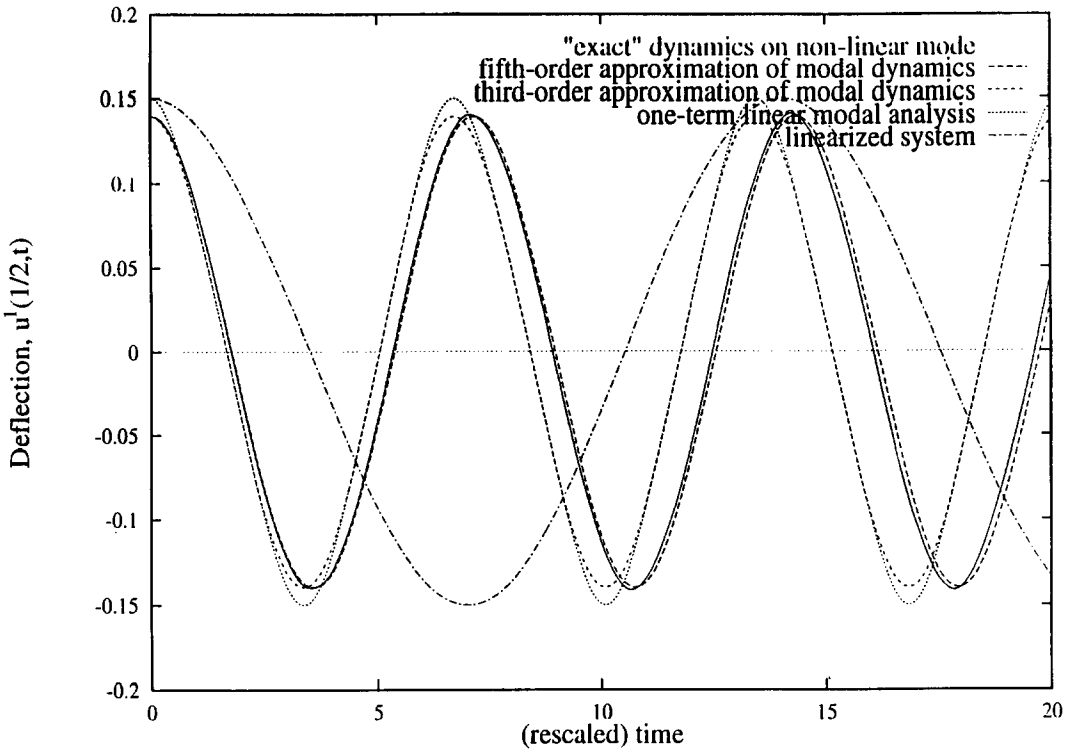

Fig. 5a. Deflection of the middle-point of the beam as obtained by the various simulations initiated on the third-order approximation of the non-linear normal mode manifold. Notice that the third order accurate modal dynamics yields the same frequency of motion (see equation (56) and (42)) as the one-term linear modal analysis, but with a more accurate amplitude.

is here no problem of convergence (in terms of the number of linear modes) or stability (in terms of time-step), which have both thoroughly been checked. Inspection of the linear mode components of the deflection and of their velocities showed that they were very smooth, which was expected, but their relative amplitudes decayed slowly with increasing mode number. This indicates the importance of the contributions of higher linear modes to the motion. This was not anticipated to occur in the "exact" simulation of the first non-linear mode motion, but rather it was expected that the contributions of the various linear modes would match those predicted by the coefficients a_6^i and a_8^i from the non-linear normal mode formulation, which decay like i^{-4} and i^{-8}, respectively (where i is the linear mode number). This larger-than-expected contribution of the higher linear modes to the motion, together with the non-periodicity of the response, mean that invariance is not achieved by the "exact" solution simulation and thus that the initial deflection shape is not a sufficiently accurate approximation of the first non-linear mode shape, yielding the contamination of the motion by other *non-linear* modes.

Another puzzling point was that the frequencies of oscillations of the non-linear normal mode simulations differed from that of the "exact" solution in a significant manner. Of course, the fifth-order non-linear dynamics presented a much better agreement with the "exact" solution than the third-order dynamics.

Those two unexpected results (the non-periodicity of the "exact" solution and the lack of agreement of the oscillation frequencies by the various approaches) suggested that the non-linear normal mode manifold was not approximated in a sufficiently accurate manner,

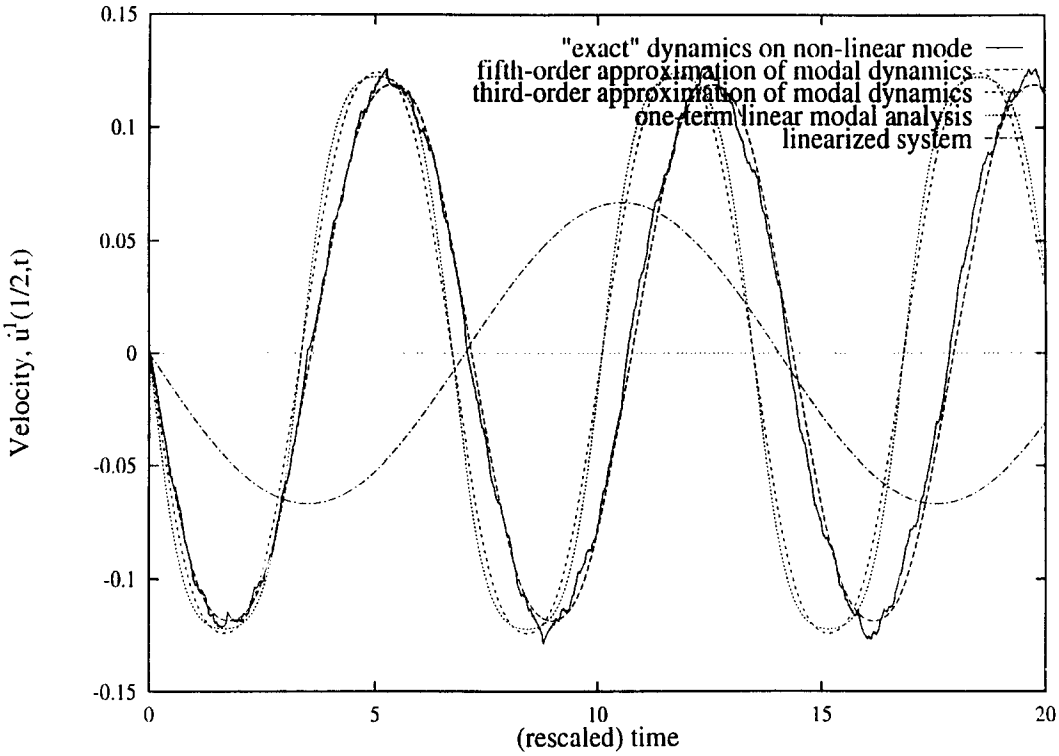

Fig. 5b. Velocity of the middle-point of the beam for the same simulations as in Figure 5a. Notice the very irregular behavior of the dynamics as determined "exactly" (motion initiated on the third-order approximation of the non-linear normal mode manifold).

and therefore, that the initial conditions were not close enough to the first non-linear normal mode.

In order to try to remedy this problem, the fifth-order approximation of the non-linear normal mode invariant manifolds was generated, following the procedure described in Section 3.2.2. This was thought to define the non-linear normal modes in a more accurate manner, hence addressing both above-mentioned problems at the same time. The geometry of the non-linear normal modes is expanded as

$$\begin{cases} X_i = a_1^i u_k + a_6^i u_k^3 + a_8^i u_k v_k^2 + a_{15}^i u_k^5 + a_{17}^i u_k^3 v_k^2 + a_{19}^i u_k v_k^4 + \cdots \\ Y_i = b_2^i v_k + b_7^i u_k^2 v_k + b_9^i v_k^3 + b_{16}^i u_k^4 v_k + b_{18}^i u_k^2 v_k^3 + b_{20}^i v_k^5 + \cdots \end{cases} \quad i = 1, \ldots, N \tag{57}$$

where only those terms consistent with synchronous motion are included. For k odd, the corresponding added coefficients are found to be

$$\begin{cases} b_{16}^i = 5a_{15}^i - 2\alpha(k\pi)^4 a_{17}^i - 4\beta a_8^i \\ b_{18}^i = 3a_{17}^i - 4\alpha(k\pi)^4 a_{19}^i \\ b_{20}^i = a_{19}^i \end{cases} \tag{58}$$

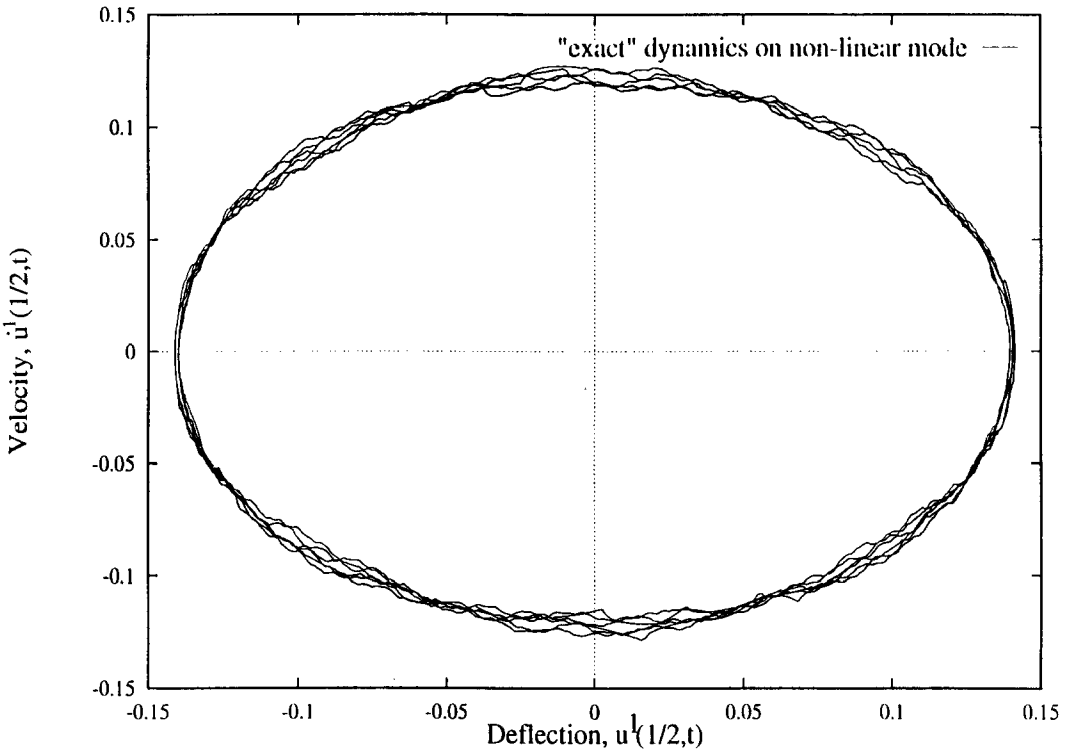

Fig. 5c. Phase-plane representation of the middle-point dynamics as determined "exactly" (motion initiated on the third-order approximation of the non-linear normal mode manifold). The irregularities in the dynamics suggest that the approximation of the non-linear normal mode manifold (on which the motion should be periodic) is not sufficiently accurate.

and

$$\begin{cases} a_{15}^i = \dfrac{-\alpha^2\pi^8(i^4-17k^4)(i^4-13k^4)\mu_1^i + 2\alpha^3\pi^{12}k^8(i^4-13k^4)\mu_2^i - 72\alpha\pi^4k^8\mu_1^i}{\Delta} \\ a_{17}^i = \dfrac{-\alpha^2\pi^8(i^4-5k^4)(i^4-13k^4)\mu_2^i + 20\alpha\pi^4(i^4-13k^4)\mu_1^i}{\Delta} \\ a_{19}^i = \dfrac{-120\mu_1^i + 6\alpha\pi^4(i^4-5k^4)\mu_2^i}{\Delta} \end{cases} \tag{59}$$

where

$$\begin{cases} \Delta = \alpha^3\pi^{12}[(i^4-5k^4)(i^4-17k^4)(i^4-13k^4)\mu_2^i + 32k^8(i^4+5k^4)] \\ \mu_1^i = 2\beta\left[3\left(\sum_{j\neq k} a_6^i \sin\left(j\frac{\pi}{2}\right)\right)\sin\left(i\frac{\pi}{2}\right) + 2a_8^i - b_7^i\right] \\ \mu_2^i = 2\beta\left[3\left(\sum_{j\neq k} a_8^i \sin\left(j\frac{\pi}{2}\right)\right)\sin\left(i\frac{\pi}{2}\right) - 22a_8^i\right]. \end{cases} \tag{60}$$

These results yield:

$$\begin{cases} \eta_k = u_k \\ \eta_i = 0 & \text{for } i \text{ even } \; i = 1, \ldots, N, \; i \neq k \\ \eta_i = a_6^i u_k^3 + a_8^i u_k v_k^2 + a_{15}^i u_k^5 \\ \qquad + a_{17}^i u_k^3 v_k^2 + a_{19}^i u_k v_k^4 + \cdots & \text{for } i \text{ odd } \; i = 1, \ldots, N, \; i \neq k \end{cases} \tag{61}$$

which in turn gives the kth non-linear normal mode as

$$u^k(s,t) = u_k \sin(k\pi s) + \sum_{\substack{i=1 \\ i \text{ odd}, i \neq k}}^{N} [a_6^i u_k^3 + a_8^i u_k v_k^2 + a_{15}^i u_k^5 + a_{17}^i u_k^3 v_k^2 + a_{19}^i u_k v_k^4] \sin(i\pi s) + \cdots \tag{62}$$

and the corresponding mode shape as

$$u_{\max}^k(s) = u_{k\max} \sin(k\pi s) + \sum_{\substack{i=1 \\ i \text{ odd}, i \neq k}}^{N} [a_6^i u_{k\max}^3 + a_{15}^i u_{k\max}^5] \sin(i\pi s) + \cdots . \tag{63}$$

Recalling the remark made earlier, the dynamics on the kth non-linear normal mode can be determined up to seventh order using a fifth-order expansion in the mode geometry. In this case, the seventh-order modal oscillators are given by:

$$\ddot{u}_k + \alpha(k\pi)^4 u_k + 2\beta u_k^3 \left[\sin\left(k\frac{\pi}{2}\right) + \left(3 \sum_{\substack{j=1 \\ j \text{ odd}, j \neq k}}^{N} [a_6^j u_k^2 + a_8^j v_k^2 + a_{15}^j u_k^4 + a_{17}^j u_k^2 v_k^2 + a_{19}^j v_k^4] \sin\left(j\frac{\pi}{2}\right) \right) + 3 \sin\left(k\frac{\pi}{2}\right) \left(\sum_{\substack{j=1 \\ j \text{ odd}, j \neq k}}^{N} [a_6^j u_k^2 + a_8^j v_k^2] \sin\left(j\frac{\pi}{2}\right)^2 \right) \right] \sin\left(k\frac{\pi}{2}\right) + \cdots = 0. \tag{64}$$

The various types of simulations were then carried out in exactly the manner described before, but by initiating the motion on the fifth-order approximation of the first non-linear normal mode invariant manifold, i.e., with the initial deflection shape given by equation (63). An additional set of simulations was also performed, using the non-linear formulation with the seventh-order dynamics governed by equation (64).

The simulation results for the dynamics of the beam's mid-point obtained by the linear modal analysis formulation are shown in Figure 6, and those obtained by the non-linear normal mode formulation are depicted in Figure 7. Observe that the "exact" solution is still not perfectly regular and periodic, but, as shown on the phase-plane plot, Figure 6b, initiating the motion on a fifth-order accurate non-linear mode shape approximation has drastically reduced

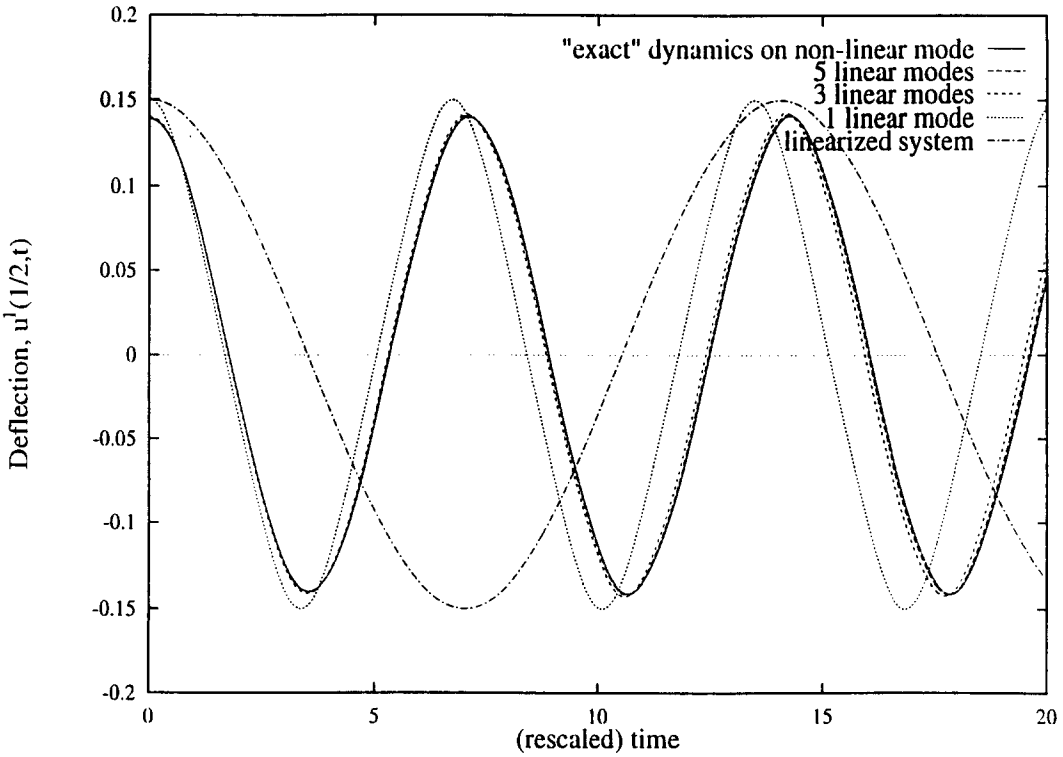

Fig. 6a. Deflection of the middle-point of the beam, obtained by various linear modal analysis simulations initiated on the fifth-order approximation of the first non-linear normal mode manifold.

the high-frequency part of the dynamics from that in Figure 5c. Besides, the superposition of the initial deflection shapes and of the "exact" shape obtained after four periods, depicted in Figure 8, shows a relatively good agreement, suggesting that the invariance of the motion in the first non-linear normal mode is nearly achieved. (Note: it would indeed be exactly achieved if one started from the exact non-linear mode instead of from an approximation of it.) Indeed, for smaller non-linearities, it was observed that since the non-linear normal mode manifold is better approximated, the invariance of the motion initiated on it is better achieved. This is not a surprise, since invariance was the cornerstone of the definition of a non-linear normal mode. This is, however, the first time it has been checked for a continuous system.

Several interesting features characterize the simulations. An important one is that the non-linear mode simulation using the seventh-order accurate dynamics agrees very well with the "exact" solution. In particular, both the amplitude and the frequency of the dynamics of the mid-point of the beam have converged towards those of the "exact" solution.

Both of the above results – invariance of the "exact" motion solution and the agreement, both in amplitude and frequency, between the "exact" solution and the non-linear normal mode simulation – confirm the validity of the invariant manifold formulation for non-linear normal modes. In the present case, given the strength of the non-linearity of the system, these invariant manifolds feature a significant non-linear geometry (i.e., non-negligible curvatures near the equilibrium point), hence necessitating high-order terms in their construction in order to capture the desired quantitative effects of the dynamics on them for the amplitudes considered.

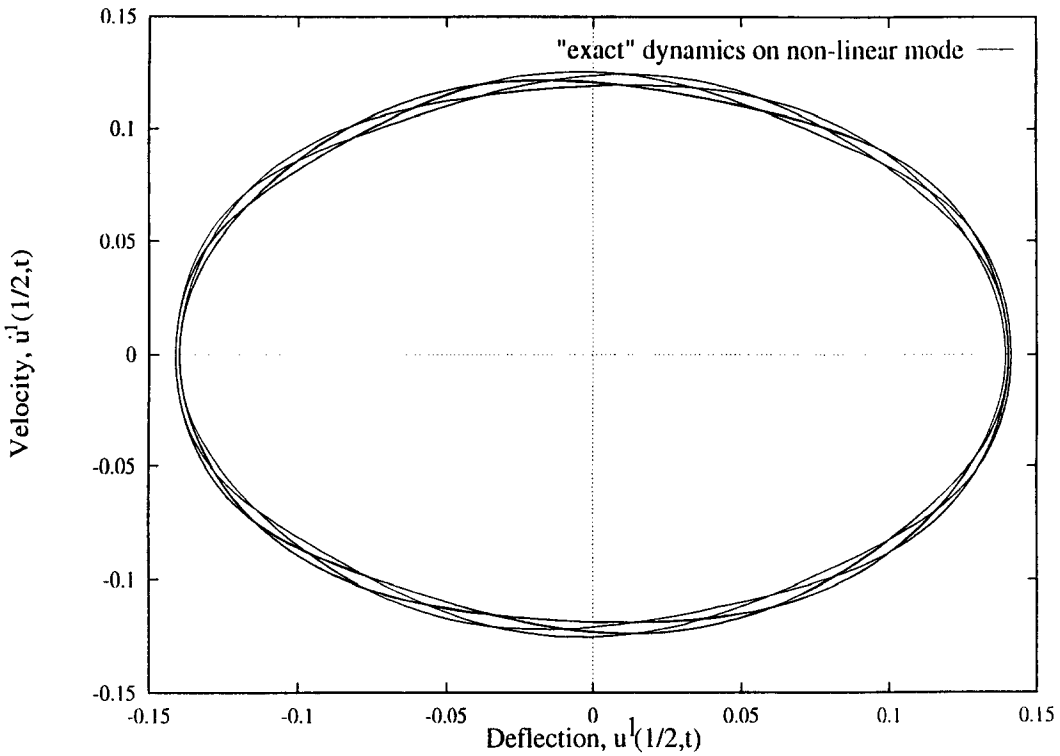

Fig. 6b. Phase-plane representation of the dynamics of the middle-point of the beam as determined "exactly" (motion initiated on fifth-order accurate first non-linear normal mode manifold). The irregularities in the dynamics have been significantly reduced compared to those in Figure 5c.

Once the approximation of the non-linear manifolds is sufficiently accurate to guarantee a legitimate use of the non-linear normal mode formulation, the accuracy of the dynamics that can legitimately be determined on them is at least one order higher – or, in the case of purely odd non-linearities, two orders higher – than that of the manifold itself, so that exact non-linear modal motions can eventually be recovered by high-order approximations of both the manifold and the dynamics. Figure 7 shows the responses obtained using the third-, fifth- and seventh-order accurate dynamics, initiated on the fifth-order accurate non-linear mode shape, as compared to the "exact" solution. Given the very good accuracy obtained by the seventh-order dynamics, it is deemed useful here to recall that it is obtained at virtually no additional cost once the fifth-order mode shape is known, hence yielding an inexpensive way of obtaining very precise quantitative features of the system's behavior. Interestingly, the numerical simulations of the third-, fifth- and seventh-order accurate non-linear modal dynamics performed on the present example show a very smooth and periodic motion for the middle-point (see the closed curve on the phase-plane plot, Figure 9), as can be expected since only a single conservative non-linear modal oscillator ODE was simulated (the consecutive recombined motion being necessarily periodic as well). For given initial conditions, those non-linear modal simulations therefore result in a periodic motion which is some known approximation (e.g, fifth or seventh order) of the exact periodic motion occurring on the exact manifold, thereby allowing the evaluation of the associated natural frequency. For small non-linearities, an analytical expression of the approximation of the frequency of motion on the non-linear normal mode manifold can be obtained from the non-linear modal oscillator

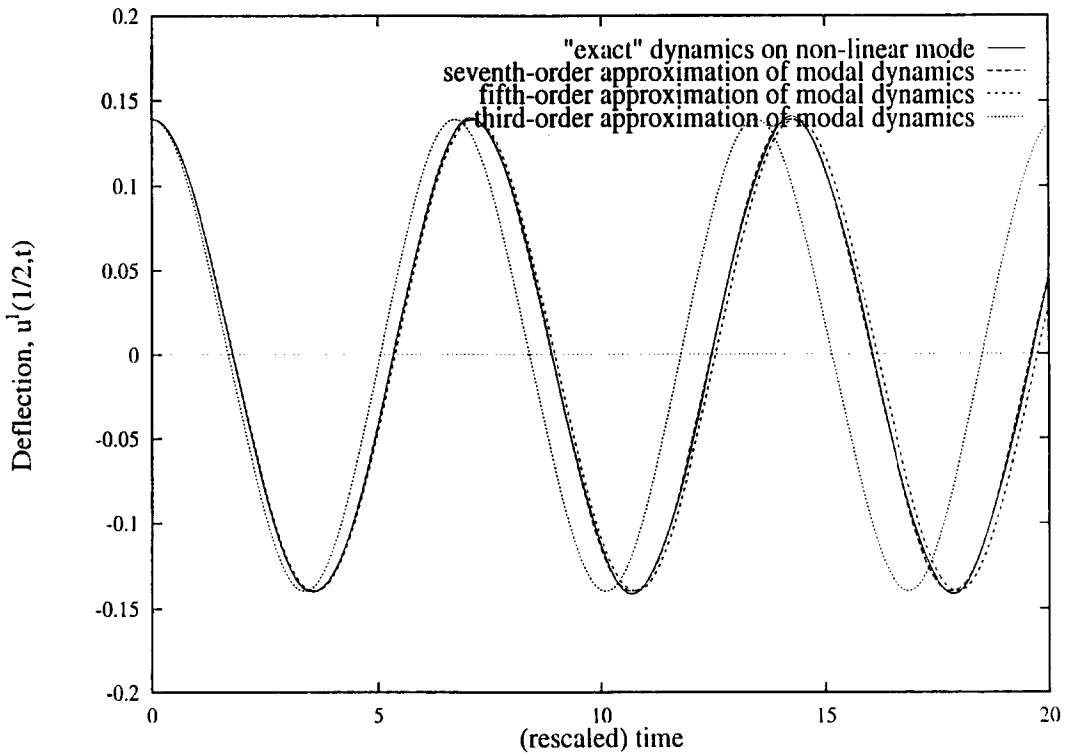

Fig. 7. Deflection of the middle-point of the beam as calculated by the various non-linear normal mode dynamics approximations (initiated on the fifth-order accurate first non-linear normal mode manifold).

equation (equation (56) or (64)) by use of traditional asymptotic techniques (e.g., Lindsted's method). For more general non-linear systems, including non-conservative ones, information on other physical quantities (e.g., damping rate) can be obtained in the same manner.

It is also interesting to compare the results obtained by a single-term linear modal analysis (equation (42) for $N = 1$) and by the non-linear mode approach using the third-order dynamics (equation (56) up to third order), both initiated on the third-order non-linear normal mode shape. Both cases correspond to the same single dynamic equation and therefore yield the same frequency of motion. However, Figure 10 shows that the non-linear mode simulation yields a much more accurate amplitude of motion, due to the recombination of the beam deflection (using equation (54)), which takes into account some of the effects of the higher linear modes. It should be re-emphasized that using only the third-order modal dynamics is pointless, since the fifth-order accurate dynamics is available. A better comparison is obtained using a fifth-order accurate simulation initiated on the third-order non-linear mode shape, and a linear modal analysis simulation using only one linear mode, both of which involve only one second-order non-linear ODE. Figure 10 then clearly illustrates the advantage of the non-linear normal mode formulation over the traditional projection of the dynamics onto a single linear mode (a widely used discretization technique) in the case of motions occurring in a pure non-linear normal mode.

For all simulations of interest initiated on the third-order accurate non-linear mode shape, Table 1 displays the error in the amplitude and the deviation in frequency (as measured from the "exact" solution initiated on the fifth-order mode shape). Similar results are gathered in

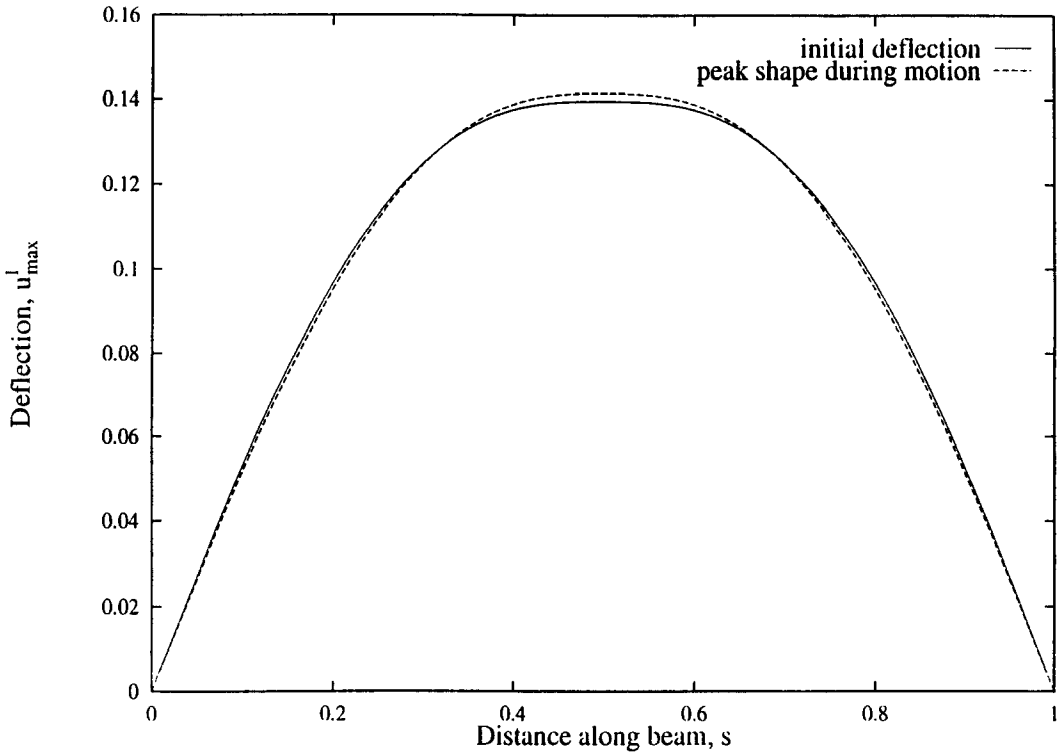

Fig. 8. Deflection shapes of the beam at $t = 0$ and at its maximum amplitude during the "exact" simulation. Note that the motion is nearly invariant.

Table 1. Errors in amplitudes and frequencies for various simulations initiated on the third-order accurate non-linear normal mode manifold approximation.

	Linear Modal Analysis				Non-Linear Normal Mode Formulation	
	linearized system	1 linear mode	3 linear modes	5 linear modes	third order dynamics	fifth order dynamics
Error in amplitude	6.8%	6.8%	1.1%	0.4%	6.7%	0.7%
Deviation from "exact" frequency	~ 96%	5.6%	0.7%	0.2%	5.6%	0.6%

Table 2 for simulations of interest initiated on the fifth-order mode shape approximation. The amplitude error measure chosen here is the ratio of the difference of the maximum amplitudes, after five periods of the motion, between a given simulation and the "exact" solution to the maximum amplitude of the "exact" solution.

One notes from Table 1 that, in order to describe the dynamics on the first non-linear normal mode manifold by linear modal analysis as accurately as by using a single non-linear normal mode with fifth-order accurate dynamics, the dynamics of at least three or five linear modes (initiated on the third-order mode shape) are required. Likewise, the very good accuracy obtained by the seventh-order dynamics simulation (initiated on the fifth-order mode shape)

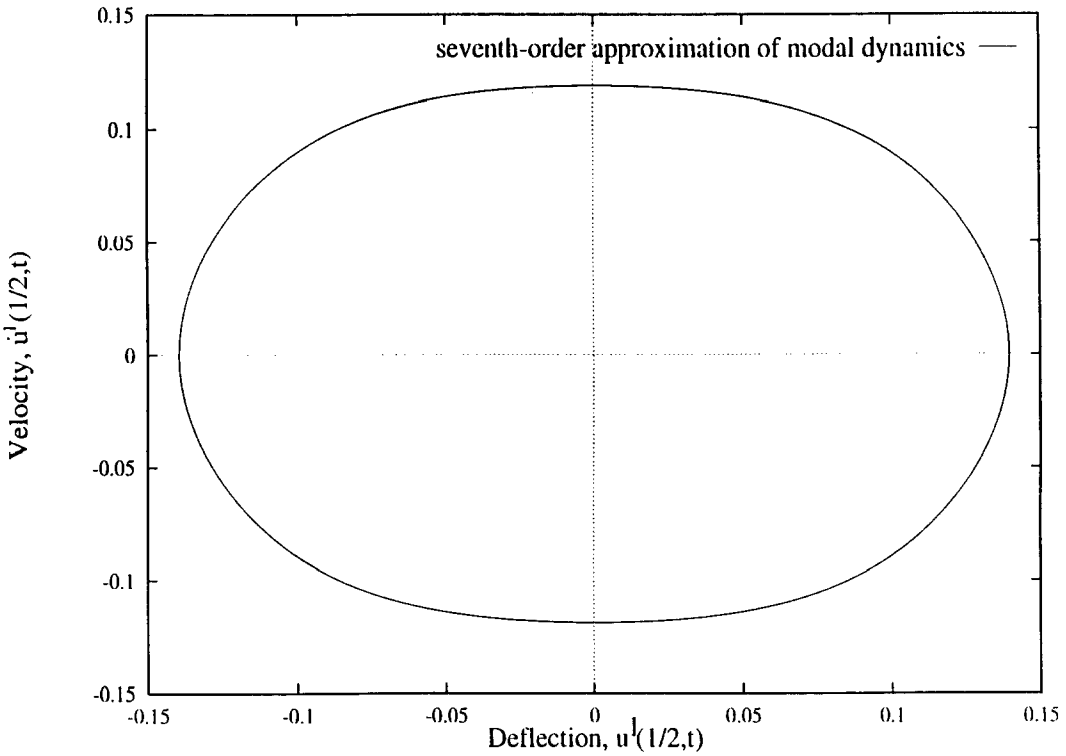

Fig. 9. State-space representation of the dynamics of the middle-point of the beam as determined by the seventh-order accurate non-linear modal dynamics.

Table 2. Errors in amplitudes and frequencies for various simulations initiated on the fifth-order accurate non-linear normal mode manifold approximation.

	Linear Modal Analysis				Non-Linear Normal Mode Formulation		
	1 linear mode	3 linear modes	5 linear modes	7 linear modes	third order dynamics	fifth order dynamics	seventh order dynamics
Error in amplitude	6.8%	1.1%	0.4%	0.2%	6.7%	0.7%	0.6%
Deviation from "exact" frequency	5.6%	0.7%	0.2%	0.1%	5.6%	0.6%	0.1%

should be emphasized, along with the fact that at least five or seven linear modes (initiated on the same mode shape approximation) are needed to achieve the same accuracy, but at a much higher computational cost. Note that there remains a significant error in amplitude between the seventh-order dynamics and the "exact" solution, and that the improvement in amplitude error between the fifth- and seventh-order accurate dynamics is only marginal (see Table 2). However, examination of Figures 5c and 6b shows that, although the "exact" solution is more regular when initiated on the fifth-order manifold approximation, the corresponding motion is still not perfectly periodic, and both phase-plane plots feature a maximum amplitude spread between 1% and 2%. Therefore, given that the amplitude error is measured at one point in time

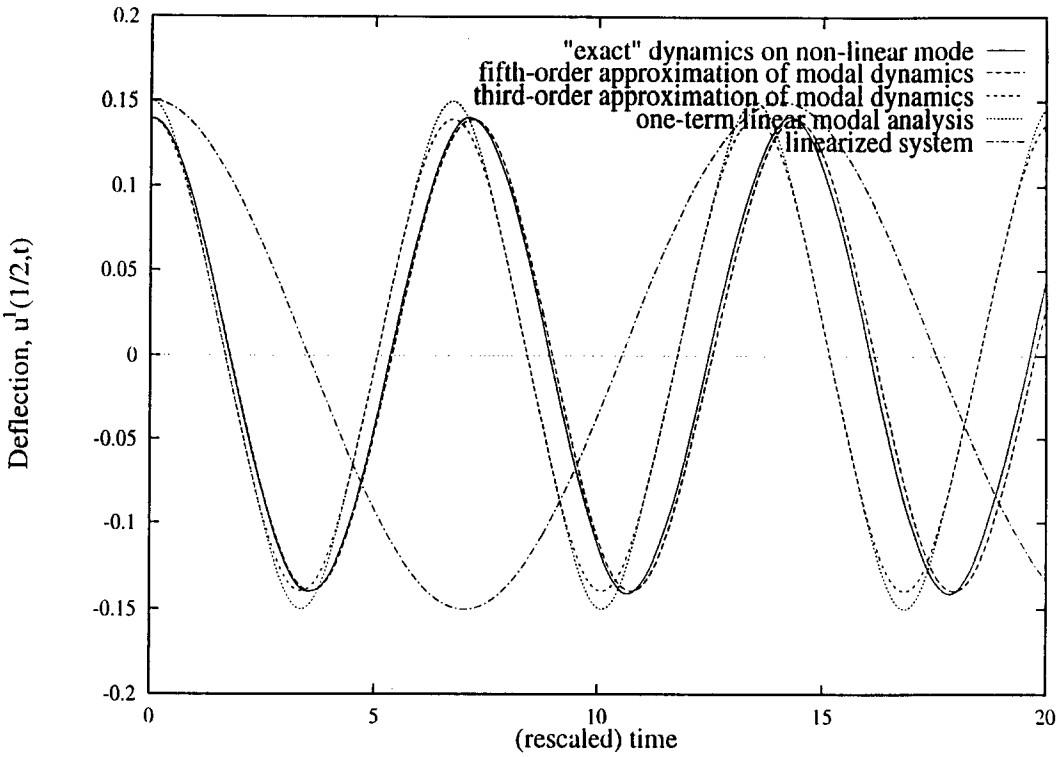

Fig. 10. Dynamics of the middle-point of the beam initiated on the third order accurate non-linear manifold, and comparison with the "exact" dynamics initiated on the fifth-order accurate non-linear modal manifold.

only, any measure of errors below 1% has no real significance. Once again, this reflects the fact that the exact geometry of the non-linear normal mode manifold is unknown. Iterating the process one more time (i.e., determining the seventh-order approximation of the manifolds' geometry, and subsequently, the ninth-order dynamics on them) would yield a more nearly closed state-space curve for the "exact" solution and a better agreement in the amplitudes of the various simulations for the given initial amplitude. Note that for both the linear modal analysis simulations and the non-linear normal mode simulations, accuracy is not noticeably improved by the use of a higher-order accuracy in the initial approximation of non-linear manifold. However, those small remaining errors are precisely those which cause the linear modal analysis simulations to behave non-smoothly (as can be observed from phase-plane plots).

Finally, the very poor result obtained by the linearized system, and the moderately good results obtained by using only one linear mode, should be emphasized, since those two methods are the most commonly employed ones when the approximate dynamic behavior of a system is sought. At this point, it is worth recalling that, once the linear modes are known, the only extra work required by the non-linear normal mode formulation is to solve a linear system of equations for the non-linear coefficients a_j^i's and b_j^i's, which is a computationally easy task. Then, only a single (second-order) non-linear ODE must be solved, followed by the recombination of the overall system motion.

4. Conclusion and Future Directions

The work presented here contains several features which significantly enlighten some aspects of the general theory of non-linear normal modes as developed in [5–8].

First, the simulations demonstrate the invariance of the non-linear normal modes, as expected, validating both the discrete and continuous formulations of this theory. Furthermore, as higher order terms are included in the analysis, the series representation of the non-linear normal modes does indeed converge to the desired invariant manifold.

Another important feature is that although the "continuous" non-linear normal mode approach is a very appealing and direct extension to continuous systems of the theory constructed for discrete systems, it may not be as reliable as it first appears, due to its dependence on the point s_0. This method was therefore left aside here.

On the other hand, the quality and the robustness of the "discretized" non-linear normal mode approach (Galerkin-type discretization using the modes of the linearized system followed by the non-linear normal mode analysis developed for discrete systems) was clearly demonstrated, since for values of parameters and initial conditions which are far from leading to a weak non-linearity, this formulation provides, in this example, good qualitative as well as *quantitative* results when one uses the fifth-order accuracy in the non-linear modal dynamics. Although presented here on a one-dimensional example, this methodology is well suited for any multi-dimensional non-linear vibratory system, since the partial differential equations of motion can always be discretized with the modes of the linearized system.

For systems with only odd order non-linearities, the dynamics on a non-linear normal mode is accurate up to an order $N+2$ when the non-linear modal manifold geometry itself is of order N. In the case of purely cubic non-linearities, the fifth-order dynamics is achieved by taking into account only the first-order corrections of the non-linearities – since there are no quadratic effects – and then the use of any order of accuracy in the dynamics below five is pointless. Likewise, for more general systems involving quadratic non-linearities, the dynamics on a non-linear normal mode can be determined up to order $N+1$ when the non-linear modal manifold geometry itself is known at order N. In such cases, the geometry of the non-linear modal manifolds may include quadratic terms, which are sufficient to capture the non-linear effects up to order three in the non-linear modal dynamics.

All the non-linear modal motion results were obtained by solving only one non-linear differential equation, whereas a traditional linear modal analysis of the non-linear system requires the solution of a set of coupled non-linear ODEs (with at least three or five modes in the present example) to provide the same level of accuracy. This may result in potentially significant savings. Also note that if one is willing to use only one differential equation for the linear modal analysis (i.e., either only one linear mode or, even worse, the linearized equation), the predictions can become very poor.

All these results suggest that, when it comes to the extension of the present non-linear mode ideas to the dynamics of several non-linear modes, that is, to non-linear modal analysis, fewer modes might be required to achieve a given level of accuracy. This is because the lower-order non-linear normal modes capture much of the influence of the higher-order linear modes, hence resulting in a reduced number of coupled non-linear ODEs to be solved. Significant modal convergence improvements are thus expected, along with corresponding computational savings. It should be emphasized at this point that this non-linear modal analysis is expected to be very easily implementable in most already existing finite element codes, hence easily

generating inexpensive, but quantitatively accurate, dynamical behaviors of engineering non-linear systems.

The non-linear normal modes as currently defined are only individually invariant (i.e., a motion started in one of them only will remain in that one for all time). This might be thought to be perfectly suited for the construction of reduced-order models, essentially by truncating the system at a finite number of non-linear normal modes, say N, and then studying the dynamics of the reduced system in a $2N$-dimensional phase-space. However, the non-linear normal manifolds, being only *individually* invariant, this process does produce undesirable coupling among the non-linear modes, which cannot be removed by the current formulation. Consequently, a non-linear modal analysis capable of systematically generating suitable invariant reduced-order models will require a generalization of the existing non-linear normal modes. In such a case, the invariance of a set of modeled non-linear modes would be necessary in order to ensure that no contamination from the ignored modes would occur. This has potentially important implications for many application areas, including modal convergence in structural dynamics and modal reduction for implementation of control systems. Future work therefore includes a complete non-linear modal analysis for discretized systems, including a study of modal convergence using both the current formulation and a generalization of it.

References

1. Meirovitch, L., *Analytical Methods in Vibrations*, Macmillan, New York, 1967.
2. Rand, R. H., 'A direct method for non-linear normal modes', *International Journal of Non-Linear Mechanics* **9**, 1974, 363–368.
3. Rosenberg, R. M., 'On non-linear vibrations of systems with many degrees of freedom', *Advances in Applied Mechanics* **9**, 1966, 155–242.
4. Vakakis, A. F., 'Analysis and identification of linear and non-linear normal modes in vibrating systems', Ph.D. dissertation, California Institute of Technology, 1990.
5. Shaw, S. W. and Pierre, C., 'Normal modes for nonlinear vibratory systems', *Journal of Sound and Vibration* **164**(1), 1993, 85–124.
6. Shaw, S. W. and Pierre, C., 'Normal modes of vibration for nonlinear continuous systems', *Journal of Sound and Vibration* **169**(3), 1994, 319–347.
7. Shaw, S. W., 'An invariant manifold approach to nonlinear normal mode of oscillation', *Journal of Nonlinear Science* **4**, 1994, 419–448.
8. Shaw, S. W. and Pierre, C., 'On nonlinear normal modes', *Proceedings of the Winter Annual Meeting of the A.S.M.E., Anaheim, California, November 1992*. DE-Vol. 50, AMD-Vol. 144.
9. Carr, J., *Application of Centre Manifold Theory*, Springer-Verlag, New York, 1981.
10. Vakakis, A. F., 'Nonsimilar normal oscillations in a strongly nonlinear discrete system', *Journal of Sound and Vibration* **158**(2), 1992, 341–361.
11. Vakakis, A. F. and Cetinkaya, C., 'Mode localization in a class of multi-degree-of-freedom systems with cyclic symmetry', *SIAM Journal on Applied Mathematics* **53**, 1993, 265–282.
12. Vakakis, A. F., 'Fundamental and subharmonic resonances in a system with a "1–1" internal resonance', *Nonlinear Dynamics* **3**, 1992, 123–143.